THE EFFECT OF DIABIETIC ACID ON THE COKING OF OXIDISED SOLVENT-EXTRACTED COAL

MARGARET TSHIMANGADZO LUDERE

Submitted in partial fulfilment of the requirements for the degree of

Master of Science

Department of Chemistry
Faculty of Natural and Agricultural Sciences
University of Pretoria
Pretoria

November 2006

ABSTRACT

Refcoal is a refined carbon source obtained by extraction of coal with dimethylformamide (DMF). During the coking process, Refcoal goes through a mesophase (fluid) stage to form an anisotropic coke. In contrast, oxidised Refcoal does not undergo such a mesophase stage during the carbonisation process. Thus it does not yield an anisotropic coke, but forms an isotropic coke. The objective of this study is to produce an anisotropic coke from oxidised Refcoal. For this purpose, diabietic acid, a hydrogen donor, was considered as a suitable additive. Coking was performed in sealed glass capillary tubes as diabietic acid proved to be volatile at the carbonisation temperature of 500 °C.

The resultant cokes were analysed using thermogravimetric analysis, Raman spectroscopy and optical microscopy. The results show that the degree of anisotropy increased with diabietic acid content (3, 5 and 10 mass %).

KEYWORDS: Refcoal, coking process, hydrogen-donating additives, anisotropic coke.

ACKNOWLEDGEMENTS

I would like to express my deepest gratitude towards the following people and institutions that contributed in making this study possible.

- My promoter, Professor Dave Morgan, for his support, encouragement and valuable advice.

- My mother for her unwavering support and belief in me.

- My daughter Vhuhwavho for her understanding, patience and love during these two long years.

- The entire staff of and all the students in the Institute of Applied Materials for their support.

- The following departments in the University of Pretoria for their help with sample analysis: Geology, Metallurgy, Engineering and Chemistry.

- Pebble Bed Modular Reactor (PBMR), THRIP and the University of Pretoria for financial assistance.

- Above all, special thanks to my Creator, God Almighty; through Him this work was possible. Luke 1:37 (*with God everything is possible*).

I dedicate this work to my late father, Mr T.W. Ludere, with great respect.

CONTENTS

ABSTRACT ..... **I**

ACKNOWLEDGEMENTS ..... **II**

LIST OF FIGURES ..... **VI**

LIST OF TABLES ..... **IX**

ABBREVIATIONS ..... **X**

CHAPTER 1: INTRODUCTION **1**

1.1 OBJECTIVES OF THE STUDY 3

CHAPTER 2: THEORETICAL BACKGROUND **5**

2.1 COAL 5

2.1.1 The formation and origin of coal 5

2.1.2 Coalification 6

2.1.3 Coal petrography 9

2.1.4 Reflectance of macerals 11

2.1.5 Structure of coal 12

2.2 SOLVENT EXTRACTION OF COAL 13

2.2.1 High-temperature solvent extraction 14

2.2.2 Factors affecting coal extraction 14

2.3 Oxidation of coal 15

2.3.1 Effect of coal oxidation on carbonisation 16

2.4 COKE 17

2.4.1 The properties of coke 18

2.4.2 Supply and demand of coke 19

2.5 GRAPHITE 19

2.5.1 Graphitic carbons (natural and synthetic graphites) 20

2.6 CARBONISATION ADDITIVES 21

2.6.1 Diabietic acid 21

2.7 CARBONISATION PROCESS 22

2.7.1 Principles of carbonisation 23

2.7.2 Classes of carbonisation 24

2.7.3 Mechanism of carbonisation 25

2.8 MESOPHASE FORMATION 31
2.8.1 Isotropic carbons 34
2.8.2 Anisotropic carbons 35
2.9 HYDROGEN TRANSFER DURING CARBONISATION 35
2.10 COMMERCIAL COKING PROCESS 36
2.10.1 Delayed coking process 37
2.10.2 Fluid coking process 38
2.11 KINETICS OF CARBONISATION 39
2.12 GRAPHITISATION 40
2.12.1 Graphitisable and non-graphitisable carbons 40
2.13 EXPERIMENTAL TECHNIQUES 42
2.13.1 Diffuse reflectance infrared Fourier transform spectroscopy 42
2.13.2 Non-Isothermal themogravimetric analysis 42
2.13.3 Nuclear magnetic resonance spectroscopy 43
2.13.4 Raman spectroscopy 43
2.13.5 X-ray diffraction 44
2.13.6 Optical microscopy 44

CHAPTER 3: EXPERIMENTAL 46

3.1 COAL SOLVENT EXTRACTION 46
3.2 OXIDATION OF REFCOAL SOLUTION 47
3.3 PREPARATION OF DIABIETIC ACID 49
3.4 CARBONISATION OF THE SAMPLES 52
3.5 SAMPLE ANALYSIS 53
3.5.1 Diffuse reflectance infrared Fourier transform spectroscopy 53
3.5.2 Nuclear magnetic resonance 53
3.5.3 X-ray diffraction 53
3.5.4 Optical microscope 54
3.5.5 Non-isothermal themogravimetric analysis 54
3.5.6 Raman spectroscopy 54

CHAPTER 4: RESULTS AND DISCUSSION 55

4.1 EXTRACTION OF THE COAL 55
4.2 THE OXIDATION OF REFCOAL 56
4.2.1 Diffuse reflectance infrared spectroscopy (DRIFT) 57

4.2.2 Nuclear magnetic resonance 58
4.3 THERMAL GRAVIMETRIC ANALYSIS (TG) 59
4.4 RAMAN SPECTROMETRY 66
4.5 X-RAY DIFFRACTION (XRD) 70
4.6 OPTICAL MICROSCOPY 71

CHAPTER 5: CONCLUSIONS 75

CHAPTER 6: REFERENCES 77

APPENDICES 85

LIST OF FIGURES

Figure 2.1: The reaction of oxygen with aromatic hydrocarbons 16
Figure 2.2: Structure of diabietic acid 22
Figure 2.3: The structure of aromatic hydrocarbons 26
Figure 2.4: Structure of aromatic hydrocarbons that are coke-formers 27
Figure 2.5: Structures and properties of char-forming aromatic hydrocarbons .. 28
Figure 2.6: The reaction product from the carbonisation of anthracene 28
Figure 2.7: Reaction products from the carbonisation of naphthalene 29
Figure 2.8: Formation of stable odd-alternate free-radical structures during carbonisation 32
Figure 2.9: Change in structure of non-graphitic mesophase conversion to graphitisable carbon 33
Figure 2.10: Influence of hydrogen transfer reactions during pyrolysis of petroleum residues on carbon formation 33
Figure 2.11: Graphitisable carbon/coke 41
Figure 2.12: Non-graphitisable carbon/coke 41
Figure 2.13: Partially graphitisable carbon/coke 41
Figure 3.1: Three litre reactor used for coal extraction 46
Figure 3.2: Gas burette used for Refcoal oxidation 48
Figure 3.3: Apparatus used for the dimerisation of abietic acid 50
Figure 3.4: Mechanistic pathway accounting for the first step in dimerisation, and by-products occurring during the acid treatment of abietic acid 51
Figure 3.5: Roto-vapor apparatus used to remove solvent 52
Figure 4.1: Progress of extraction of coal at 94 °C 55
Figure 4.2: Volume of oxygen consumed on treating 200 ml of Refcoal solution at ambient temperature 56
Figure 4.3: DRIFT spectrum of oxidised Refcoals 57
Figure 4.4(a): ^{1}H NMR spectra of abietic acid 58
Figure 4.4(b): ^{1}H NMR spectra of the abietic acid dimer 59
Figure 4.5(a): TG and DTG curves of neat abietic and diabietic acid obtained in N_2. 60

Figure 4.5(b): TG and DTG curves obtained in N_2 for of diabietic acid carbonised in a sealed quartz tube at 680 °C for 5 h 61
Figure 4.5(c): TG and DTG curves of neat coal (precursor) obtained in N_2 61
Figure 4.6(a): Comparison of the TG and DTG curves obtained in N_2 for (A) Refcoal and (B) Refcoal carbonised at 680 °C for 5 h 62
Figure 4.6(b): TG and DTG curves obtained in N_2 for (A) oxidised Refcoal and (B) oxidised Refcoal carbonised at 680 °C for 5 h 62
Figure 4.6(c): TG and DTG curves obtained in N_2 for (A) oxidised Refcoal (B) oxidised Refcoal carbonised at 680 °C for 5 h 63
Figure 4.6(d): TG and DTG curves obtained in N_2 for (A) oxidised Refcoal and (B) oxidised Refcoal carbonised at 680 °C for 5 h 63
Figure 4.6(e): TG and DTG curves obtained in N_2 for (A) oxidised Refcoal and (B) oxidised Refcoal carbonised at 680 °C for 5 h 64
Figure 4.7(a): Summary of TG and DTG curves obtained in N_2 for oxidised Refcoal 64
Figure 4.7(b): Summary of TG and DTG curves obtained in N_2 for carbonised oxidised Refcoals at 680 °C for 5 h 65
Figure 4.8: TG and DTG curves obtained in N_2 for Refcoal and oxidised Refcoal carbonised at 680 °C for 5 h 66
Figure 4.9(a): Raman spectra of oxidised Refcoal cokes 67
Figure 4.9(b): Raman spectra of oxidised Refcoal cokes treated with 3% diabietic acid 67
Figure 4.9(c): Raman spectra of oxidised Refcoal cokes treated with 5% diabietic acid 68
Figure 4.9(d): Raman spectra of oxidised Refcoal cokes treated with 10% diabietic acid 68
Figure 4.10: Intensity ratios of the G- to D-peaks observed in the Raman spectra of oxidised Refcoal cokes 69
Figure 4.11: The XRD spectra of carbonised (A) diabietic acid and (B) oxidised Refcoal with 10% diabietic acid and graphite powder 70
Figure 4.12: Optical micrograph of carbonised diabietic acid 71
Figure 4.13(a): Optical micrograph of oxidised Refcoal cokes 72

Figure 4.13(b): Optical micrograph of oxidised Refcoal cokes treated with 3% diabietic acid 73
Figure 4.13(c): Optical micrograph of oxidised Refcoal cokes treated with 5 % diabietic acid 73
Figure 4.13(d): Optical micrograph of oxidised Refcoal cokes treated with 10% diabietic acid 74
Figure A1: Structure of graphite 87

LIST OF TABLES

Table A.1: Properties of nuclear-grade graphite 85
Table A.2: Physical properties of graphite 85
Table A.3: Uses of coal extracts 86
Table A.4: Ultimate analysis of Tshikondeni coal 86
Table A.5: Proximate analysis 86
Table A.6: Progress of extraction with DMF 88
Table A.7: Data for the oxidation of the Refcoal 89
Table A.8: Infrared spectral regions 91
Table A.9: NMR shift classifications 91
Table A.10: Operation parameters of X-ray powder diffraction 92
Table A.11: Operation parameters of Raman spectroscope 92

ABBREVIATIONS

Å	angstrom
CHC	hexachlorocyclohexane
DMF	dimethylformamide
DRIFT	diffuse reflectance infrared Fourier transform
DSC	differential scanning calorimetry
DTA	differential thermal analysis
H_2SO_4	sulphuric acid
HF	hydrofluoric acid
HTGR	high-temperature gas-cooled reactor
kPa	kilopascal
kV	kilovolt
ℓ	litre
mm	millimetre
MW	megawatt
NaOH	sodium hydroxide
nm	nanometre
NMR	nuclear magnetic resonance spectroscopy
º	degree
ºC	degree Celsius
PAH	polyaromatic hydrocarbons
PBMR	pebble bed modular reactor
QI	quinoline insoluble
temp.	temperature
TGA	themogravimetric analysis
XRD	X-ray diffraction
θ	theta
Ω	omega

CHAPTER 1: INTRODUCTION

South African power utility giant Eskom is experiencing short, sharp electricity demand peaks, especially during winter, and it is very difficult to adapt to these with the existing large thermal power stations. Electricity demand is also expected to exceed capacity between 2003 and 2010 in South Africa. Almost 90% of electricity in South Africa is generated in coal-fired power stations, 5% is produced by one large nuclear power station (Koeberg near Cape Town), while another 5% is provided by hydroelectric and pumped storage schemes.

Since 1993 Eskom has been investigating pebble bed technology as part of its integrated electricity planning process. It has come up with a project to establish a Pebble Bed Modular Reactor (PBMR) as a future source of base-load energy, with the intention of developing and marketing small-scale, high-temperature reactors both locally and internationally.

The PBMR is a high-temperature gas-cooled reactor (HTGR) of 110 MW capacity per module and is fuelled by several hundred thousand graphite-uranium oxide pebbles, each the size of a tennis ball. The helium coolant passes through a gas turbine to generate electricity with high efficiency, and returns to the reactor in a closed loop. Each pebble passes through the reactor about ten times before needing replacement, which is carried out continuously without the reactor having to be shut down. Four modules would fit inside a football stadium and the design lifetime is 40 years. (Greyvenstein, 2003).

High-temperature reactor technology was developed in Germany in the early 1980s and such a reactor operated for two years before it was shut down permanently as a result of mechanical problems. The PBMR is advantageous because it is cheap to build, economical to operate, has a short construction period of about 24 months, does not emit any greenhouse gases and, lastly, is radiologically safe (Nicholls, 2000 and PBMR website).

Eskom believes that there will be a market both in South Africa and the rest of the world for PBMRs, 30 of which could be built within 12 to 15 years. The implementation of this nuclear reactor will be of great benefit to South Africa and neighbouring countries because it will generate enough low-cost electricity to meet the needs and will create sustainable job opportunities.

The PBMR consists of a vertical steel pressure vessel, 6 m in diameter and 20 m high. This pressure vessel is lined with a layer of graphite bricks. This graphite layer serves as an outer reflector for the neutrons generated by the nuclear reaction and as a passive heat-transfer medium. Vertical holes are drilled into the graphite brick lining to house the control elements. This graphite reflector encloses the core (Koster *et al*,. 2003). The core is the region of the reactor in which the nuclear reaction takes place. The PBMR core is 3.7 m in diameter and 9.0 m in height. When fully loaded, the core would contain 436 000 fuel spheres.

The geometry of the fuel region is annular and located around a central graphite column. The latter serves as an additional nuclear reflector. The nuclear reaction takes place in the fuel annulus. Helium is used as a coolant, because it does not change during the operation range of the PBMR and the neutron absorption cross-section of helium is very small, which implies that the reactivity of the core will not increase due to a change in the state of the coolant (PBMR website).

PBMR fuel consists of moulded graphite spheres containing coated fuel particles. The fuel particles (kernels) are composed of uranium dioxide. They are coated with a layer of porous carbon and two high-density layers of pyrolytic carbon (a very dense form of heat-treated carbon), with a layer of silicon carbide in between (Nicholls, 2000). The porous carbon accommodates any mechanical changes that the kernel may go through during the lifetime of the fuel and the fission products released from the kernel. The pyrolytic carbon and silicon carbide layers provide an impenetrable barrier, thus containing the fuel and the radioactive products that result from the nuclear reactions (Morgan, 2002 and PBMR website).

The PBMR pebbles contain uranium enriched to about 8% in ^{235}U. The ^{235}U is the isotope of uranium that undergoes the fission reaction in the core. The reactor is

continuously refilled from the top with fresh or reusable fuel, while used fuel is removed from the bottom after each cycle through the reactor. A fuel sphere will last about three years (Nicholls, 2000 and Morgan, 2002).

With regard to safety, the reactor is described as being safe because the silicon carbide shell around the uranium oxide beads is able to retain all fission products at a higher temperature of about 2 000 °C. The PBMR does not have any risk of releasing radioactive elements. The reactor is cooled by helium and if the coolant gas were to stop flowing, the reactor would warm up to 1 330 ^{o}C – this is the point at which the negative coefficient of criticality would bring the chain reaction to a close. Fission products from radioactive decay would continue to heat the fuel up to a temperature of 1 600 °C, the heat lost by the reactor shell would balance the heat production and then the reactor core would slowly cool down. There would be no release of radioactive fission products below this temperature.

During graphitisation, carbon loses much of its impurity load, except for the carbide-forming elements, which tend to come off slowly at higher temperatures. Carbon graphite is chosen as one of the best materials for nuclear fission reactors due to its high moderating efficiency as required for nuclear reaction and its low absorption cross-section for neutrons; it also has a high sublimation point and oxidises slowly at higher temperatures. The graphite blocks must be of high strength and highly isotropic to give the best dimensional stability under irradiation and to obtain uniform thermal expansion in all directions. The graphite used for fission reactors and fusion systems is derived from blocks of petroleum or pitch cokes.

1.1 OBJECTIVES OF THE STUDY

The main objective of this study was to produce anisotropic cokes suitable for being properly graphitised to produce pure synthetic graphite for nuclear use. These cokes were prepared from Refcoal and oxidised Refcoal. (Refcoal is a refined carbon source obtained by extraction of coal with dimethylformamide.) The Refcoal solution was oxidised and compared with the unoxidised Refcoal.

Since oxidised Refcoal does not go through a fluid (mesophase) stage during the carbonisation (coking) process because of the higher content of oxygen, then it does not form anisotropic coke during this process. Diabietic acid was then used as a hydrogen donor additive during carbonisation of the oxidised and unoxidised coal it also show great improvement on the anisotropic texture. In order to get anisotropic coke, coal oxidation should be avoided.

The coal samples were heated in sealed glass capillary tubes. All carbonised end-products were characterised by Raman spectrometry, optical microscopy and thermogravimetric analysis (TGA).

CHAPTER 2: THEORETICAL BACKGROUND

2.1 COAL

Coal is the most abundant of our three major fossil fuels, namely oil, coal and gas. It can be burned to provide heat and light, and to generate electricity. It contains a number of chemicals, which are for various purposes (Wilson and Wells, 1950). It is also the basis of various manufacturing processes (plastics, pharmaceutical products, iron and steel, aluminium and many other materials in daily use). From coal we get dyes, floorings, antiseptics and fertilisers. Currently, coal is needed to make graphite for coating fuel pebbles in order to generate electricity in a high-temperature nuclear reactor. This makes it a very important natural resource and much effort is still being expended on making the most of it (Granfield and Buckman, 1978). It can be used either as a heating and steam-raising fuel, or carbonised to form cokes and chars, or converted into synthetic gaseous and liquid hydrocarbons. It is a major source of carbon materials.

Coal is usually a dark colour, although geologically younger deposits of brown coal have a brownish-red colour. The colour, lustre and fracture vary with rank, type and grade. Coal is the result of the combined biological, chemical and physical degradation of plant matter accumulated over geological ages. The relative amounts of remaining plant parts lead to different types of coal, which are sometimes termed banded, splint, non-banded, hard or soft, lignite, sub-bituminous, bituminous or anthracite (Wilson and Wells, 1950).

2.1.1 The formation and origin of coal

Coal is not just another form of carbon, such as graphite and diamond, but is highly amorphous. It is a fossil that has physical and chemical properties determined by its geographical location. Different coals vary significantly due to their geographical location and age. It is believed to originate predominantly from plant matter and results from the action of temperature and pressure on plant debris.

About three million years ago in certain parts of the world there were warm and humid climatic conditions that enhanced the growth of huge tropical ferns and giant trees, which grew and died in vast swamp areas. The dead trees rested in boggy waters, which killed bacteria and excluded oxygen. Thus the dead plants decomposed to produce a peat-like material. During prospecting and analysis, fossilised plant remains are found in major coal deposits. In fact, fossilised spores have an important role in identifying coal seams.

The vegetation continued to grow for many millenniums, eventually forming vast thick peat beds, which later turned into coal. Since the rate of subsidence of the coal basins was not constant, the cycle of swamp followed by submersion was repeated a number of times, which resulted in the build-up of a sequence of horizontal bands of peat and inorganic, sedimentary rocks. This process formed a biochemical stage, which was the first stage.

There was then a subsequent intervention in the bands of peat by the action of temperature and pressure during the second stage, thus resulting in the formation of the coals found today. This is called the geochemical stage. As time continued, there was a further alteration in the horizontal coal seams as they became folded, tilted and eroded.

2.1.2 Coalification

Coalification is the term given to the development of the series of different types of coals. This process takes place in two stages, namely biochemical degradation and geochemical degradation (Valkovic, 1983).

2.1.2.1 Biochemical degradation

Biochemical degradation involves the chemical decomposition of botanical matter or plants. Various organisms assist this degradation. There are four processes to which the botanical matter may be subjected after death:

- rotting
- mouldering
- putrefaction

- peatification.

For all these processes to occur there must be participation by aerobic or anaerobic bacteria, fungi, larvae, worms and various enzymes, and they must take place under partial action of water, mineral admixtures and gases (Snyman, 1976). In tropical environments this process is faster because the warm, moist conditions are ideal for the organisms that assist in the decomposition of botanical matter, such as fungi and bacteria (Snyman, 1976). However, the vegetation growth is more rapid because it relies mostly on the increased rate of botanical matter decomposition. In tropical conditions, high rates of evaporation need to be coupled with high precipitation to maintain plant growth and peat accumulation.

In cooler climate conditions, the growth rate of vegetation may be cyclical in nature and slower because the supporting organisms in the decomposition of botanical matter are not favoured under those conditions (Falcon, 1978). The overlying principle is that the less ideal the conditions are for fungi and bacteria, the slower the vegetation growth rate and therefore the slower the rate of biochemical degradation. Aerobic microorganisms are able to exist only in the presence of free oxygen. Anaerobic microorganisms take the necessary oxygen from the chemical compounds. The decay of plant material usually occurs first by the action of aerobic agents with access to air. Subsequently, the anaerobic microorganisms continue the decomposition process, particularly when the access to air is limited or interrupted altogether.

2.1.2.2 Geochemical degradation

Geochemical degradation is the stage that follows the biochemical degradation stage. This stage is caused by the conditions of burial of the degraded botanical matter and it actually occurs in the absence of organisms. The heat that is radiated to the matter because of the high temperature of the Earth's crust, tectonic heat and pressure alter the buried degradation product, thereby changing the chemistry and structure of the organic material. In fact, the principal factors that control geochemical degradation are temperature, pressure, volume and time (Snyman, 1976).

Temperature, which may act for a long time, is a very important factor, providing it is not too high. The assumption behind this belief is that temperatures of 100–150 ºC over a long period will appreciably affect the coalification process (Starch *et al.*, 1982).

Geochemical coalification results in increasing coal ranking. Water is squeezed out and the pore size (porosity) is reduced as the pressure increases, and then oxygen and hydrogen are released during the thermal cracking. Water and carbon dioxide are the first products released. A rapid fall in porosity in the early stages of coalification is used as a detector to indicate the formation of brown coal or peat. When the ranking of coal reaches medium volatile bituminous coal, demethanation begins (Snyman, 1976).

The development of lignite, brown coal, bituminous coal and anthracite is observed just after the formation of peat and it is a result of slow inorganic maturing. The end-products of geochemical degradation are solid, coaly causto-bioliths (brown coal, bituminous coal and anthracite) and the gas that escapes from the coal during coalification (Starch *et al.,* 1982). It has been found that the end-products of coalification depend on the state of the organic matter at the end of the biochemical phase and on the degree of degradation attained in the geochemical phase.

Coalification is believed to be an exothermic process, with the heat released during coalification decreasing with the degree of carbonisation, which disappears completely in the stage of critical metamorphism. Once the exothermic process ceases, coalification also stops. The geothermal gradient affects the degree of coalification and an accurate measurement of the degree of coalification is a sensitive indicator of the maximum temperature to which a coal seam was exposed. The degree of coalification can also be indicated by the optical properties of a coal, such as the reflectance of vitrinite, which are dependent on the chemical composition of that coal. Measurement of coal reflectance is a rapid method of characterisation and is largely uninfluenced by petrographic variations. Starch *et al.,* 1982 have shown that there is a good general relationship between reflectance and aromaticity. The physical changes are observed as the ranking progresses through bituminous to anthracite.

During geochemical coalification, a decrease in moisture and an increase in specific gravity are believed to have occurred as a result of increasing compaction with depth. However, the rapid tectonic movement occurring along faults and over thrusts during earthquakes is reported to occasionally cause a local rise in rank due to the concentration of frictional heat. These frictional forces are suspected to cause severe metamorphism of coal. Because these forces are accompanied by high temperatures, they may have caused the transformation of anthracite to graphite.

2.1.3 Coal petrography

There is a standard method of characterising the organic (maceral) and inorganic (mineral) constituents of coal (O'brien *et al*., 2003). From these data the rank and composition of a coal can be determined. Geologists use these data to understand the processes of coal deposition, and chemists use the data to evaluate the coking potential of a coal. Coal macerals are optically homogenous, discrete microscopic constituents of the organic fraction of coals, and they constitute the building blocks of coal (Scott, 2002). They are identified and classified on the basis of their morphology, source material, colour/level of reflectivity and nature of formation (*Encyclopedia of Physical Science and Technology, 1987)*

Macerals differ because they represent different parts of the original plant material and microorganisms. The most widely used classification system for macerals is the Stopes-Heerlen system (*Encyclopedia of chemical technology, 1993*). This system classifies macerals into three groups based on their optical and chemical properties.

The three basic groups of macerals are the *vitrinite* group derived from coalified woody tissue, the *liptinite* group derived from the resinous and waxy parts of plants, and the *inertinite* group derived from charred and biochemically altered plant cell-wall material. Macerals in coal are characterised by their reflectance of incident light, as well as their hardness (*Encyclopedia of Physical Science and Technology, 1987*).

2.1.3.1 Vitrinite macerals

Vitrinite macerals are derived from the cell-wall material (woody tissue) of plants, which are chemically composed of polymers, cellulose and lignin. The vitrinite group is the most abundant group and commonly makes up 50 to 90% of most North American coals (Carpenter, 1988). However, most Gondwanaland coals and some western Canadian coals are vitrinite-poor. The inertinite macerals dominate in these coals.

2.1.3.2 Liptinite macerals

The liptinite macerals are derived from the waxy and resinous parts of plants, such as spores, cuticles and resins, which are resistant to weathering and diagenesis. They generally make up about 5 to 15% of most North American coals (American Society for Testing and Materials, 1979). They are usually more abundant in the Appalachian coals than any other U.S. coals, except the cannel and boghead types in which they dominate. At a reflectance of 1.35–1.40, most of the liptinite macerals disappear from coal (Schapiro, 1960). Cannel and boghead coals are petrographically distinguished from humic coals by both their maceral composition and texture. They have an abundance of liptinite macerals (sporinite in cannels and alginite in bogheads) and a paucity of vitrinite and inertinite macerals (International Committee for Coal Petrology, 1963).

The outstanding petrographic feature of the liptinite group of macerals is that they all have a reflectance that is lower than that of the vitrinite macerals in the same coal (Stopes, 1935). This group of macerals is very sensitive to advanced coalification and the liptinite macerals begin to disappear in coals of medium-volatile rank and are absent in coals of low-volatile rank. When liptinite macerals are present in a coal, they tend to retain their original plant form and thus they are usually *plant fossils* or phyterals. The phyteral nature of the liptinite macerals is the main basis on which they are classified.

2.1.3.3 Inertinite macerals

The inertinite macerals are derived from plant material that has been strongly altered and degraded during the peat stage of coal formation. For example, fossil charcoal is the inertinite maceral called fusinite. In most North American coals the inertinite macerals range from less than 5% to 40%, with the highest amounts generally occurring in Appalachian coals (International Committee for Coal Petrology, 1963). However, the inertinite macerals can make up over 50 to 70% of some western Canadian coals.

The inertinite macerals have the highest reflectance of all the macerals and are distinguished by their relative reflectance and structures.

2.1.4 Reflectance of macerals

The reflectance of macerals or other particles in coal is described by Collin (1984) as the proportion of directly incident light (expressed as a percentage) that is reflected from a plane polished surface under specific conditions of illumination. This property is related to the aromaticity of the organic compounds in the coal and it increases progressively for all the macerals as the rank of coal increases. Its measurement is taken by dry objectives or by a water or oil immersion technique using oil with a refractive index of 1.518 at 23 $^{\circ}$C and an incident light wavelength of 546 nm. The reflectance so obtained is calculated from equation (1) (Collin, 1984).

$$R = \frac{Rs \bullet A}{As} \qquad (1)$$

Where

R = reflectance of coal maceral

Rs = reflectance of a calibration standard

A = deflection induced by the standard substance

As = deflection of galvanometer.

The reflectance, R, is related to the optical properties of the other material and the immersion medium by the following Beer's equation (2):

$$R = \frac{(n - n)^2 + n^2 k^2}{(n - n_1^2) + n^2 k^2} \qquad (2)$$

Where

n = refractive index of reflecting material

k = absorption index of reflecting material

n_1 = reflecting index of medium in which the measurement is made.

2.1.5 Structure of coal

Coal is a three-dimensional structure, a crossed-linked viscoelastic glassy macromolecular solid that is permeated by low-molecular-weight material (Yoondo *et al.*, 1983; Dekker, 1981; and Valkovic, 1983). This model is based on the assumption that coals behave similarly to cross-linked polymeric networks (Martinez-Escandell *et al.*, 1999). The theory developed in an attempt to describe the properties, such as the degree of cross-linking and glass transition temperatures, of these networks and was extended to coal.

Part of the evidence for this theory is that coals behave as elastic, not plastic, solids. This suggests that the cross-linkages are covalently fixed. Given *et al*. (in Marsh, 1989) reported a macromolecular/molecular two-phase system – the host/guest or rigid and mobile phase model. The model suggests that a substantial proportion of the organic part of coal – the mobile phase or *guest* – is composed of a low-molecular-weight phase, physically trapped within an immobile phase or *host* of high molecular weight (Marsh, 1989). The latter is extensively cross-linked.

Hydrogen bonding is reported to form the major force that holds the minerals at the maceral boundaries (Mohindar *et al*,. 1988) The minerals are believed to hold the coal's inorganic and organic aggregates together and are potential sites of further hydrogen bonding. Since the structure of coal shows many possible sites for hydrogen bonding, breaking the hydrogen bonds along the maceral boundaries could result in the separation of mineral matter from the coal matrix. The coal's macromolecular structure is made up of condensed aromatic rings forming large units

bridged or cross-linked by aliphatic and/or ether groups, which confer on them a certain structural order. The removal of the cross-links by a solvent-reagent mixture, with subsequent heating to high temperature, facilitates the reorganisation of the aromatic units into a graphite-like structure (Gonzalez *et al.*, 2002).

The macromolecular model of coal revealed condensed rings of an aromatic system, consisting of two to four rings connected by bridging units and substituted by naphthenic rings, alkyl substituents and phenolic groups. The bridges contain C-C and C-O bonds, which provide some flexibility in a cross-linked structure (Bodily *et al.*, 1986).

2.2 SOLVENT EXTRACTION OF COAL

Solvent extraction has been developed as a technique for investigating coal composition and producing waxes, resins or other coal derivatives of potential commercial value. Coal extraction or dissolution is another way of purifying coal, in which the inorganic mineral components are separated from the organic components. Mineral matter in coal consists largely of aluminosilicate compounds, such as kaolinite and clays, in conjunction with quartz (Sharma and Singh, 1995; Giri and Sharma, 2000). Mineral matter is extracted from coal with different solvents, alkalis and acids.

Coal has a cross-linked three-dimensional network gel structure. The coal molecules are closely packed in coal particles (Maya *et al.*, 1995). Different physical forces, such as hydrogen bonds, London and Van der Waal's forces, pi-pi and charge transfer interactions, etc., act as intermolecular forces between the coal molecules (Yokono *et al.*, 1983).

During the extraction process, the solvent must diffuse not only into the micropores of the solid coal matrix without any limitation, but also inside the coal to swell it. It is during swelling that the solvent breaks the intermolecular forces between coal molecules, such as hydrogen bonding, Van der Waal's and London forces, and other charge-transfer and pi-pi interactions, makes its own bonds with the coal molecules

and extracts the coal. Thus the solvent must diffuse inside the solid coal molecule and then diffuse out with the soluble coal molecules (Mohindar *et al*, 1988).

2.2.1 High-temperature solvent extraction

Coal is extracted with dimethylformamide (DMF) plus sodium hydroxide (NaOH). The ratio of solvent: coal: sodium hydroxide is 1000:100:10; extraction is done for 5 to 6 hours at 94 $^{\circ}$C. The process is conducted in an oil or water bath jacketed reactor under nitrogen. Nitrogen is used to prevent oxidation of the solution. By taking samples of the solution at different time intervals, centrifuging them, diluting them with DMF in a volumetric flask, and then measuring the absorbance at 600 nm, the rate of extraction can be monitored. The insoluble materials are separated from the solution by centrifugation. The extraction efficiency is described by the proportion of carbon removed from the coal, calculated from equation (3).

$$\%\ C\ Extraction = \frac{\left(Mass\ of\ C\ in\ coal\ before\ extraction - Mass\ of\ C\ in\ coal\ after\ extraction\right)}{Mass\ of\ C\ in\ coal\ before\ extraction}$$

Where C is Carbon

2.2.2 Factors affecting coal extraction

The extraction or dissolution of coal using organic solvents produces a decrease in impurities as the carbon content of coal increases. About 90% of the carbon content can be dissolved, depending on which solvent is used. Previous work shows that various solvents give different dissolution percentages (Renganathan 1988). The solubility of coal in organic solvents depends on a number of process parameters. The parameters that have an effect on the solubility of coal are the temperature at which extraction is carried out and the time taken to do the extraction. Even coal particle size, moisture and oxygen can have some effects on coal dissolution.

2.2.2.1 Temperature

The extractability of coal using solvents such as amines, alcohols, alkanes, aromatics and alkenes was found to increase with an increase in the boiling point within that class of solvents (Sharma and Singh, 1995). As the temperature increases, the coal

becomes thermally disintegrated; the solvent vapours are also superheated at temperatures above boiling point. This will increase the diffusion of solvent vapours inside the intermolecular spaces in the coal particles. Intermolecular physical bonding can be weakened under diffusion pressure in liquid and vapour form.

Mostly, diffusion and mass transfer control the solvent extraction in this area. As the solvent boils, the kinetic energy of the system increases, and the molecular collisions and impingements also increase due to the increase in molecular vibrations. The expanded solvent generates more space for the accommodation of the coal molecules. Thus successive sequential extractions would result in enhanced extraction. If the chemical nature of the solvents is the same, then the higher the temperature, the greater will be the dissociation of coal molecules caused by the breaking of intermolecular forces by heat energy, in addition to the dissociation of coal molecules caused by the attraction and interaction with organic solvents (Kara and Ceylan., 1988).

The macromolecular structure of coal can undergo a change after interaction with the solvents. After extraction of the coal and removal of the solvent from the swollen coal, the macromolecular cross-linked chain segments shrink back and rearrange to acquire a lower free energy configuration. If the coal could be treated with a number of solvents having different chemical characters, successively, then the associative forces present in the cross-linked gel structure of the coal could be broken stepwise and a large amount of the coal could be rendered extractable.

Since coal has a multi-functional group structure, the different molecules would be placed in coal aggregates with different physical linkages having their own respective functional group associations. The solvent must create in itself sufficient interstitial spaces (or gaps) to accommodate large coal molecules.

2.3 OXIDATION OF COAL

The structure of coal is considered to be a three-dimensional macromolecular network composed of aromatic and hydro-aromatic units, cross-linked by ether bonds, methylenic groups, hydrogen bonds and Van der Waal's interactions (Starch

et al., 1982). Since coal is a highly heterogeneous substance, low-temperature oxidation of coal would be a complex process.

The early stages of coal oxidation involve the attack of molecular oxygen on certain aliphatic bonds, such as methylene in OR groups, in order to produce peroxides and hydroperoxides (Teng *et al.*, 1997). The latter then decomposes to produce oxygenated functional groups, mainly carbonyls, esters and acids. During coal oxidation the oxygen-to-carbon (O/C) ratio increases, while there is a reduction in the hydrogen-to-carbon (H/C) ratio (Lopez *et al.*, 1998). Aromaticity increases with oxidation and this shows that the non-aromatic part, such as the benzylic position, of the coal is the first to be oxidised to produce carbonyl groups and carboxylic acids (Figure 2.1).

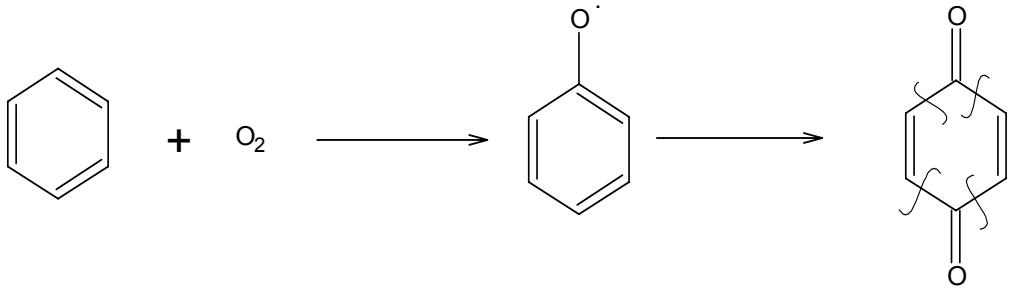

Figure 2.1: The reaction of oxygen with aromatic hydrocarbons

2.3.1 Effect of coal oxidation on carbonisation

During carbonisation coal softens, melts and resolidifies to form coke when heated in the absence of air. All these processes are very important for the production of coke, but they are all affected by the oxidation of coal, which is known to affect the properties of coke produced through carbonisation. Carbonisation is also used to reduce the caking properties in other coal utilisation processes such as gasification, combustion and the production of activated carbon (Valkovic, 1983).

Coal oxidation also decreases the extractability of the solvent, reduces the softening and swelling tendencies, and decreases the total yield of volatiles during carbonization (Teng *et al.*, 1997). The decrease in solvent extractability is caused by

the reduction of transferable hydrogen during oxidation. The weight loss during carbonisation under nitrogen also decreases because of this oxidation process. Oxygen is believed to reduce drastically the graphitisation of pitch. It has also been found to inhibit mesophase development.

X-ray analysis of oxygen-containing aromatics has shown that oxygen substitution could result in both well and poorly ordered graphite (Collin, 1984). Mild oxidation has been shown to reduce dehydrogenative polymerisation without necessarily leading to a less graphitic final structure. The decrease in final graphitisability through extensive oxidation of the starting material was reported to be attributable to the formation of quinones which pyrolyse with the loss of CO to give radicals.

2.4 COKE

Coke is the hard, porous residue left after the destructive distillation of organic matter, especially coal and petroleum residuals. It is used mainly as a fuel, a reductant and a support for other raw materials in iron-making blast furnaces. It is also used in the chemical industry, in non-ferrous smelters and in the form of speciality carbons such as carbon bricks, electrodes, etc. Blast furnace and smelter cokes are normally made from coal, whereas electrode carbons and carbon bricks are commonly made from petroleum residuals. Coke is black to silver-grey and has a metallic lustre. It is composed largely of carbon, usually about 92%; most of the remainder is ash. When used as a fuel, it has a high heating value. Coal carbonisation is an extremely complicated art.

Coke was first produced as a by-product in the manufacture of illuminating gas. The growth of the steel industry, however, produced a rising demand for metallurgical coke, so that coke is now one of the chief products manufactured.

The earliest method of coking coal started when coal began to replace wood as a raw material in the charcoal pile. It was natural that coke production should begin in piles or mounds with flues similar to those used for charcoal production. These flues were filled with wood, which was lighted and which started burning the coal. When most of the volatile elements in the coal had been driven off, the flames would die

down; the fire would then be partly covered with coal dust, and the heap scattered with water.

The coking of coal in a 'beehive' oven (named because of its shape) was developed later as the demand for coke increased and the sites of coke production became more permanent. As in open-air coking, no effort was made to recover the valuable gas and tar that were by-products of the process. Beehive ovens have now been almost entirely supplanted by the modern by-product coke ovens. These ovens, usually arranged in batteries of about 60, are narrow vertical chambers with silica-brick walls, heated by burning gas flowing between adjoining ovens. Each oven is charged through an opening in the top with anywhere from 10 to about 20 tons of coal, which is heated to temperatures as high as 1 480 ºC for about 17 hours. During this period the gases from the oven are collected through another opening in the top. The coal tar is condensed by contact with water in a hydraulic main, while the gas, after being scrubbed with water to remove ammonia and with oil to remove benzene, is used to heat the ovens. At the end of the coking period the red-hot coke is forced by a ram out of the oven directly into a car that carries it to the quenching hood, where it is sprinkled with water. The emptying process takes only about 3 minutes, so that the oven is ready for recharging with little loss of heat.

Petroleum cokes represent the second-largest source of cokes used in the carbon industry. Unlike cokes produced from coal, petroleum cokes are derived from the residuals of petroleum refining. Several petroleum-coking methods have been developed. The preferred coking processes used nowadays are delayed coking, followed by fluid and flexi-coking.

2.4.1 The properties of coke

Coke used in iron-making furnaces has three primary functions:

1. Coke is the fuel that is burned in the blast furnace. The heat produced by the burning of coke provides the energy needed for the different reactions in the process, including the melting of iron raw materials and increasing the

temperature of liquid iron to that required for its downstream processing into steel.

2. The combustion and gasification of the coke produces the gases that act as reducing agents to remove oxygen from iron raw materials in the blast furnace.

3. Coke is the only blast furnace material that remains solid at high temperature and can exist in the lower portions of the furnace. It is thus able to support the rest of the material and to provide an upwards path for the gases and a path for the downward-falling iron droplets to meet and interact.

2.4.2 Supply and demand of coke

By far the most coke is produced from slot-type by-product coke ovens. Total coke production worldwide was about 378 X 10^6 t in 1990 and this tonnage has remained stable for the last two decades.

The demand for blast furnace coke worldwide has decreased over the past decade. Blast furnaces for hot metal production (pig iron) increased by about 4% from 1980 to 1990, and coke production decreased by about 2% over the same time period. As the practice of injecting coal into blast furnaces increases, an additional reduction in the rate of coke production is expected. Coke production rates have fallen by 4% in some countries that have aggressively adopted coal-injection techniques (*Encyclopedia of Physical Science and Technology., 1987)*.

Coke production is expected to continue decreasing unless new coke-making facilities are constructed, because the effective production capacities of coke plants decreases as the coke plants age. This situation is of great concern in North America where the majority of coke plants are over 25 years old and the economic life-spans of conventional coke batteries average about 20 years.

2.5 GRAPHITE

Graphite is one of the three allotropic forms of carbon; the other forms are diamond and buckminsterfullerene. Graphite is also called *plumbago* or *black lead*.

It occurs in nature as a mineral, invariably containing impurities. It is widely distributed all over the world. Important deposits are found in England, Siberia, Madagascar, Mexico, Sri Lanka, Canada and numerous localities in the United States (Hugh, 1993). Graphite is made artificially by baking a mixture of petroleum coke and coal tar pitch at 950 °C for 11 to 13 weeks, then transferring the baked product to electric graphitising furnaces and heating it to about 2 800 °C for 4 or 5 weeks (Marsh, 1989). Most of the graphitising process takes place because of the high temperature, but the process is also a refining step as almost all the metal oxide impurities in the raw carbon are reduced to metals and vaporised.

Graphite is chemically the same as diamond, but it differs greatly from that mineral in most of its physical properties. Graphite is black, opaque and metallic in lustre and has a relative density of 2.09 to 2.2. As it is extremely soft (hardness 1 to 2), it smears anything with which it comes into contact and feels greasy or slippery to the touch (*Encyclopedia of chemical technology., 1994)*. It crystallises in the hexagonal system, not as well-developed crystals but as scales or large irregular masses. It is the only non-metal that is a good conductor of electricity; unlike other conductors of electricity, it is a poor conductor of heat. The centres of ‘lead’ pencils contain no lead but are made of graphite mixed with clay. Graphite is used as electrodes in electrochemical industries where corrosive gases are given off; for electric furnaces that reach extremely high temperatures; as a lubricant – either by itself or mixed with grease, oil or water; in crucibles that must withstand extremely high temperatures; and in industrial paints (*Encyclopedia of chemical technology., 1994)*. It has also been used as a moderator in nuclear reactors, where material of the highest purity obtainable slows down the neutrons created in the fission process that produces nuclear energy, without capturing them.

2.5.1 Graphitic carbons (natural and synthetic graphites)

A graphitic carbon consists of elemental carbon in the form of graphite, irrespective of structural defects. Graphite is an allotropic form of the element carbon consisting of layers of hexagonally arranged carbon atoms in a planar condensing-ring system. The layers are stacked parallel to each other and the chemical bonds within the

layers are covalently bonded with sp^2 hybridisations. The mixing of two or more atomic orbitals such as the p,s orbital is called *hybridisation*. The carbon atoms in ethane form sp^3 hybridisation, in ethene sp^2 hybridisation and in ethyne, sp hybridisation.

Natural graphite is a mineral that occurs in nature and it is mined, processed and used in a variety of applications as lubricants, seals, insulation, fillers and refractories. It consists of graphitic carbon and has excellent crystallinity. Some graphites show a high degree of perfection, e.g. Tyconderoga graphite, but some of the mercantile natural graphite mined is 'chip graphite' containing other minerals.

Synthetic or artificial graphite is a material consisting mainly of graphitic carbon that has been obtained by means of graphitisation heat treatment of non-graphitic carbon at temperatures above 2 500 °C (Marsh, 1989). The most common synthetic graphites are usually manufactured as composites in which ground petroleum coke is mixed into a paste with a coal tar pitch and then heat treated to around 1 200 °C –- 1 400°C in a calcining step in order to coke the pitch and drive all volatile material from the petroleum coke. Heating further to 2 500 °C – 3 000 °C causes an ordering of the carbon atoms to graphitise the mixture into true graphite (Marsh *et al.,* 1980).

The biggest industrial use of synthetic graphite is in the massive electrodes used in carbon-arc furnaces to melt steel. It is also used in the manufacture of carbon anodes for aluminium production (Marsh *et al.,* 1997). Other applications are in battery electrodes, refractories, nuclear reactors, and even in medical devices such as replacement heart valves.

2.6 CARBONISATION ADDITIVES

2.6.1 Diabietic acid

Abietic acid is a major component of the oleoresin synthesised by many conifers and constitutes a major class of environmental toxic compounds with potential health hazards to animals, humans and plants (Aranda and Villalaín, 1997). In this study abietic acid was considered as a hydrogen-donating substance because it is a

cheap, readily available by-product of the paper-making industry and is the major component of Tall oil rosin (Riddell *et al*., 1997).

Diabietic acid (Figure 2.2) is obtained from abietic acid, which is extracted from N-grade rosin. It has excellent film-forming properties and therefore has a wide application in paints, varnishes and cosmetics (Ramani *et al.*, 1996). It is prepared by dimerisation of abietic acid using sulphuric acid. Glycerol esters of abietic acid are used in fluid surgical dressings to form a hydrophobic film over a wound surface to protect it from water. Abietic acid and its derivatives can be used as micro-encapsulating materials for pharmaceutical formulations.

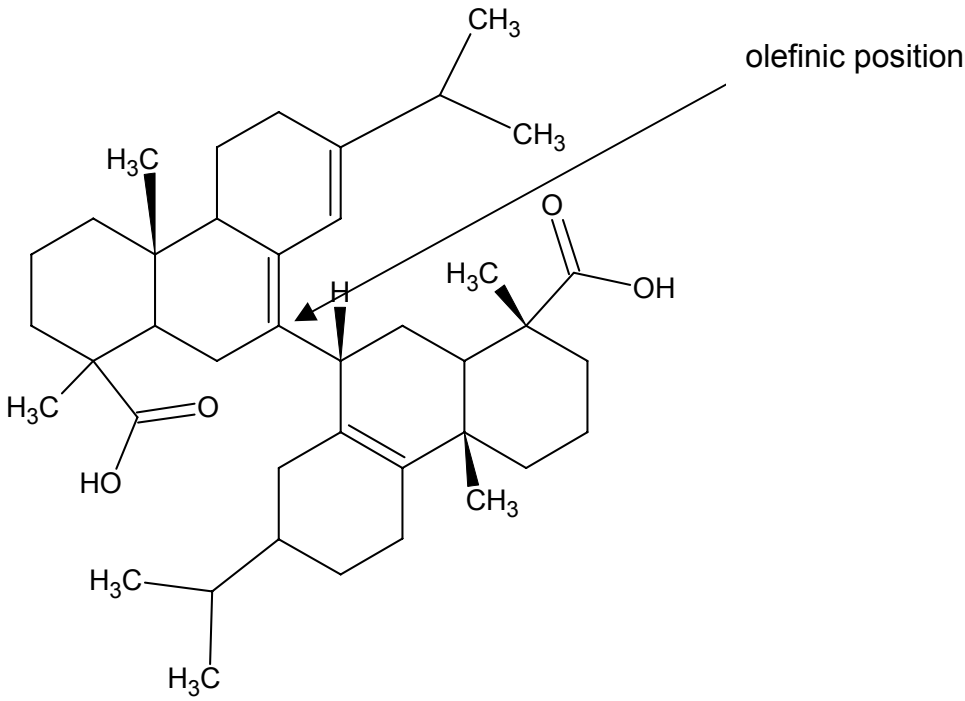

Figure 2.2: Structure of diabietic acid

2.7 CARBONISATION PROCESS

The carbonisation process, also known as *pyrolysis*, can be defined as the step in which the organic precursor is transformed into a material that consists largely of carbon. This process happens in the absence of oxygen.

2.7.1 Principles of carbonisation

Carbonisation is basically a heating cycle. During carbonisation the precursor undergoes destructive distillation in the absence of air and produces a solid, porous, carbonaceous residue – coke – which remains in the furnace, and also evolves a number of volatile products, which escape. The precursor is heated slowly in a reducing or inert environment, over a range of temperatures that vary with the nature of the particular precursor and may extend to 1 300 °C. The organic material is decomposed into a carbon residue and the volatile compounds diffuse into the atmosphere. The process is complex and several reactions may take at the same time, such as dehydrogenation, condensation and isomerisation. The carbon content of the residue is a function of the nature of the precursor and the pyrolysis temperature. It usually exceeds 90 weight % at 900 °C and 99 weight % at 1 300 °C (Pierson, 1993).

The diffusion of the volatile compounds into the atmosphere is a critical step and must occur slowly to prevent interruption and breakage of the carbon network. As a result, carbonisation is usually a slow process. Its duration can vary considerably, depending on the composition of the end-product, the type of precursor, the thickness of the material, and other factors. Some carbonisation processes, such as those used in the production of large electrodes, can last for several weeks (Pierson, 1993). Others are shorter, such as the carbonisation process to produce carbon fibres, since these fibres have a small cross-section and the diffusion path is short.

2.7.1.1 Characteristics of carbonised materials

After carbonisation, the residual material is essentially all carbon. However, its structure has a little graphitic order and consists of an aggregate of small crystallites, each formed of a few graphite layer planes with some degree of parallelism and usually with many imperfections.

The carbonised material is often called ‘amorphous’ or ‘baked’ carbon. It is without long-range crystalline order and the deviation of the interatomic distances of the carbon atoms (from the perfect graphite crystal) is greater than 5% in both the basal

plane (*ab* directions) and between planes (c direction), as determined by X-ray diffraction (Pierson, 1993).

Amorphous carbon is hard, abrasion-resistant, brittle and has low thermal and electrical conductivities. In a few cases, these characteristics are desirable and amorphous carbon is found in applications such as contacts, pantographs, current collectors and brushes for operation on flush mica commutators, as well as in special types of carbon-carbon. In most instances, however, amorphous carbon is only the intermediate stage in the manufacture of synthetic graphite products.

2.7.2 Classes of carbonisation

There are three classes of carbonisation: high-temperature, medium-temperature and low-temperature carbonisation.

2.7.2.1 Low-temperature carbonisation

The low-temperature process is usually carried out with the carbonisation temperature in the range of 450 to 700 °C. The main objective of the low-temperature process is to produce a high yield of reactive coke with a high tar yield. These cokes are black and porous, containing 8 to 20% volatile matter, and they are used for smokeless domestic fuels or industrial purposes. They may be produced in lump or powder form. The powder is briquetted. The solid yield on a dry basis ranges from 70 to 80%, with a tar yield of 7 to 10%. The specific gravity of the tars is 1.07 (Gibson and Gregory, 2000).

During carbonisation, as the temperature increases from 400 to 500 °C the bulk of the volatile matter is removed. The volatile products consist of gas, ammonia, tar and light oil. The gas composition is predominantly methane and hydrogen. Low-temperature carbonisation provides a high tar yield and a low gas yield as compared with the high-temperature carbonisation process. The cokes are weaker than high-temperature cokes. The chars from the low-temperature process are more reactive, which is important in some applications. The yield of gas from the low-temperature process is much lower than it is from the by-products of coking and the oils differ materially in characteristics from high-temperature oils.

2.7.2.2 Medium-temperature carbonisation

This process usually takes place between temperatures of 700 and 900 °C. Generally, the aim is to produce reactive cokes with a high gas yield. The process has been used for the production of so-called 'town gas'. The solid product yield ranges from 55 to 60%, with a tar yield between 4.5 and 5.5%. The solid product has a volatile matter content on a dry ash-free basis of 2 to 8% (Gibson and Gregory, 2000).

The gas is an important fuel. Most of the ammonia is converted to ammonium sulphate, one of the most important nitrogen fertilisers, and from the light oil and tar are produced benzene, toluene, xylene, phenol, naphthalene, and roofing tar and other tar products, both crude and refined. The volatiles from the coke ovens are termed *by-products*.

2.7.2.3 High-temperature carbonisation

In high-temperature coking the final temperature of the coke is usually above 900 °C and the temperature in the heating flues of the retorts is still higher. This process is used for the production of metallurgical coke for use in iron-making blast furnaces and beehive coke ovens, and for the manufacture of gas in by-product coke ovens, gas ovens and gas retorts (Gibson and Gregory, 2000). The high-temperature cokes produced in this country are burned in factories and used in other industrial applications and as a domestic fuel. High-temperature coke is the fuel used in blast furnaces and usually more than 90% of the coke consumed in these operations is manufactured in by-product ovens (Koch *et al*, 1995).

2.7.3 Mechanism of carbonisation

2.7.3.1 Carbonisation mechanism of aromatic hydrocarbons

The graphite precursors can be divided into two major classes*: (a) aromatic hydrocarbons* and *(b) polymers,* each with different carbonisation characteristics.

Structure of aromatic hydrocarbons

The term *hydrocarbon* refers to an organic compound that contains only carbon and hydrogen. *Aromatics* are hydrocarbons that can be described by the presence of at least one benzene ring. Aromatics have a graphite-like structure and graphite is often considered to be the parent of all these compounds. The structure of benzene is shown in Figure 2.3 below:

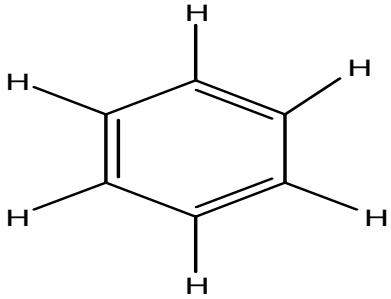

Figure 2.3: The structure of aromatic hydrocarbons

The structures of the aromatic coke formers and char formers are shown in Figures 2.4 and 2.5 respectively. Some of the most important aromatics are the following:

Anthracene is a linear, planar molecule with three benzene rings. In an autoclave at approximately 450 °C, it begins to lose the hydrogen atoms in the 9,10 positions. Free radicals are formed and condensed into gradually larger, planar molecules and then heated coke is formed (Delhaés, 1979).

Phenethracene is a branched, planar isomer of anthracene. It carbonises to a char in a manner similar to anthracene, but with a lower yield.

Biphenyl has two benzene rings connected by a single carbon-carbon bond. It is non-planar, with free rotation around this bond. It carbonises to a char.

Naphthalene, $C_{10}H_8$

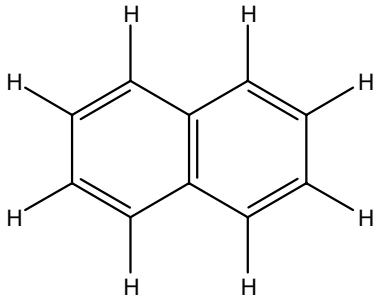

Anthracene, $C_{14}H_{10}$

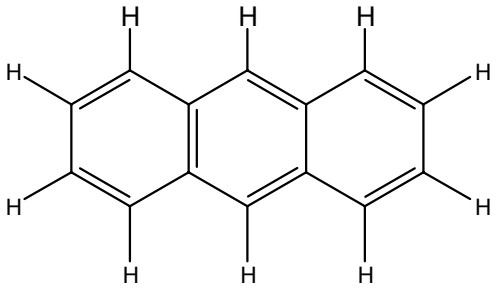

Acenaphthalene, $C_{12}H_8$

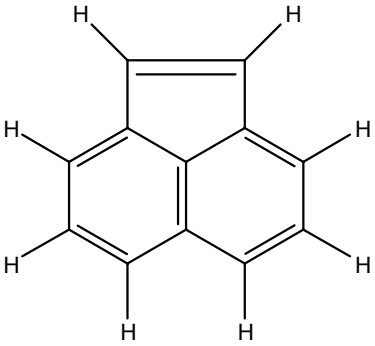

Figure 2.4: Structure of aromatic hydrocarbons that are coke-formers

Phenanthracene, $C_{14}H_{10}$

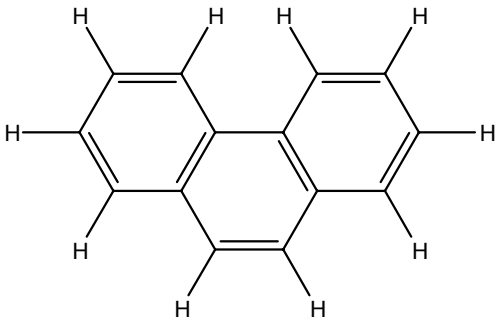

Biphenyl, $C_{12}H_{10}$

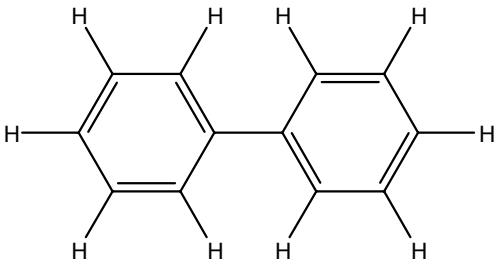

Figure 2.5: Structures and properties of char-forming aromatic hydrocarbons

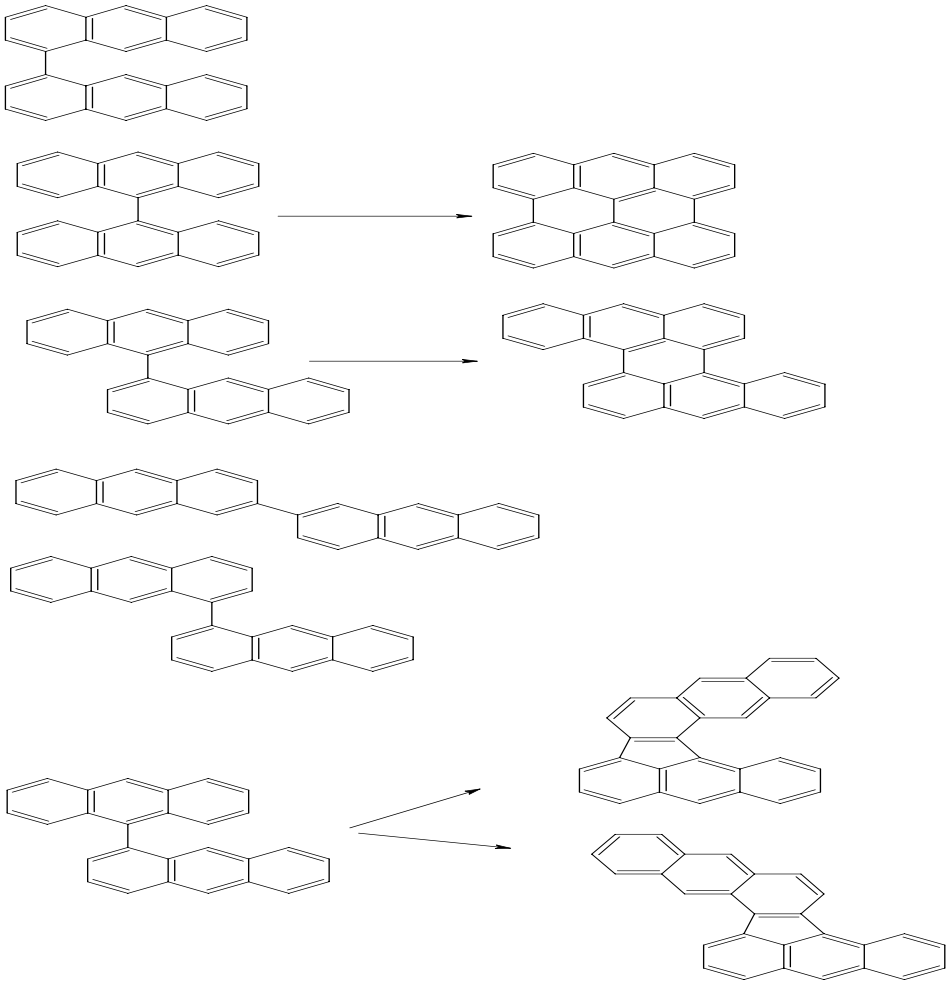

Figure 2.6: The reaction product from the carbonisation of anthracene

(Grint *et al.,* 1985)

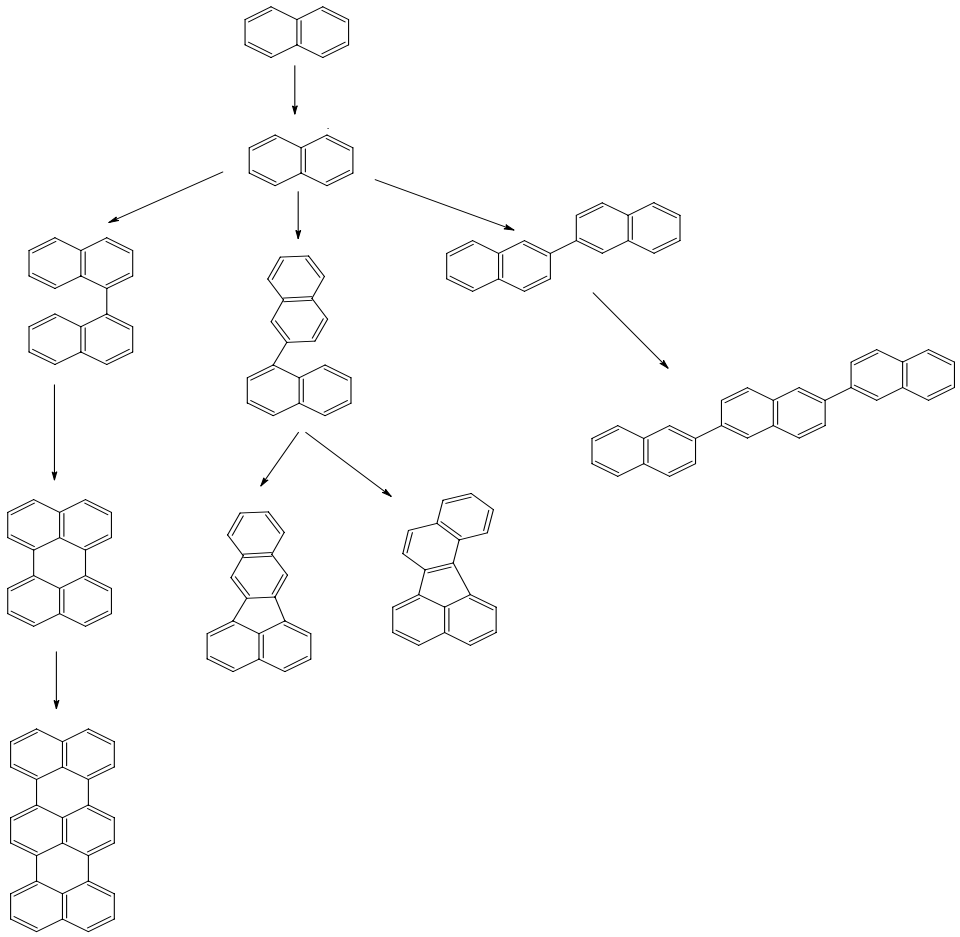

Figure 2.7: Reaction products from the carbonisation of naphthalene (Grint A *et al.,* 1985)

2.7.3.2 The carbonisation mechanism of polyaromatic (PAH) hydrocarbons

This mechanism includes the following steps:

1. Two PAH molecules disproportionate into one hydro-aromatic molecule and one free-radical molecule.
2. The free-radical molecules condense into aromatics with higher molecular weight
3. The hydro-aromatic molecules cleave to produce liquid- and gas-phase species.

Coal-tar pitch and petroleum pitch are complex mixtures of polyaromatic hydrocarbons (PAH) and are widely used in the moulded graphite industry. Coal-tar pitch is the solid residue remaining after the distillation of coal tar. It is predominantly

composed of aromatic- and heterocyclic-hydrocarbon compounds. Its composition varies depending on the nature of the coal tar. It is a solid at room temperature and has a broad softening range (up to 150 ºC) and no well-defined melting point. The carbon yield is not fixed and differs with the composition (Pierson, 1993).

Petroleum pitch is the residue from the distillation of petroleum fractions. Like coal-tar pitch, it has a varying composition, consisting mostly of aromatic and alkyl-substituted aromatic hydrocarbons. A solid at room temperature, it also has a broad softening range and no well-defined melting point. The formation of its mesophase is related to the chemical constituents and the asphaltene fractions. Coal-tar and petroleum pitches do not crystallise during cooling but can be considered as supercooled liquids. Single hydrocarbons of interest as precursor materials are anthracene, phenatrene and naphthalene (Figures 2.6.and 2.7).

2.7.3.3 Carbonisation mechanisms of coal

There are several necessary conditions for coal to be transformed into coke. The conditions include a heat supply and enclosure or blanketing to prevent oxygen contact with the coal particles during the carbonisation process. In conventional vertical coke ovens these conditions are readily met. The heat is supplied from gas-burning flues located within the walls of each oven. Loading the coal into the oven and pushing the product (coke) from the oven are accomplished through by the openings in the oven which can be sealed to prevent the incursion of air (Mantell, 1968).

During the heating process, coal molecules undergo many reactions. The primary reaction involves pyrolysis and the formation of radicals having a lower molecular weight than in the original coal. Some of the radicals are enriched with hydrogen from the liquid and gaseous products. In other reactions some radicals form more stable substances with a higher molecular weight and lower hydrogen content.

When coal is loaded into the hot coke oven, the coal particles adjust to the temperature of the coke oven walls and doors, and begin to devolatilise and soften immediately. The softened particles sinter into each other and are further

devolatilised. A layer of fully sintered coal particles is formed. Apart from these hot surfaces, there are successive layers of coal in various stages of softening, melting fusing and resolidifying. This arrangement results in the existence of an envelope of plastic coal, which continues to move inward, away from the heated surfaces, until the plastic envelope (*mesophase*) converges at the centre of the coal charge. The plastic envelope represents a barrier to gas movement (Gibson and Gregory, 2000).

2.8 MESOPHASE FORMATION

It is already known that an ordering process occurs during carbonisation, between the softening and the resolidification of certain coking coals and pitches. The general carbonisation mechanism of polyaromatic hydrocarbons is relatively simple, at least in theory, since it proceeds by the breaking of the carbon-hydrogen bonds and the removal of the hydrogen. Some of these hydrocarbons first go through an intermediate liquid or plastic stage, which occurs at temperatures above roughly 400 $^{\circ}$C (Pierson, 1993). This stage is the so-called *mesophase* in which the material shows the optical birefringence characteristic of disc-like, nematic liquid crystals, i.e. crystals that have a lamellar arrangement with the long axes in parallel lines (Masashi, 2000).

Mesophases are intermediates between liquid and crystal. Since coal is a solid material during the early stages of carbonisation, it has to pass through a mesophase state to form graphitisable material (Marsh *et al.*, 1980). The mechanisms of mesophase growth are influenced by two factors. The first factor is the molecular weight of the material, whereby a high molecular weight of the material delays mesophase formation and the steric structures do not favour liquid crystal growth. The second factor is the chemical molecular composition of the starting material (Machnikowski *et al*, 2002).

During this melting stage, condensation takes place and large polyaromatic molecules are formed with a molecular weight averaging 1 000 (Koch *et al*, 1995). These polycyclic liquid crystals gradually increase in size to build up more common Van der Waal's attractions to start promoting their alignment and form pre-cokes or *green cokes* (Bundy *et al.*, 1996). The green cokes still retain from 6 to 20% volatile

matter at 600 °C. These volatiles are gradually removed as the temperature is raised. During the mesophase process, coke shows the optical characteristics of a liquid. The optical texture shows the flow domain of a highly fluid liquid. As the mesophase flows, it establishes and annihilates the gross defects within the liquid system.

The hydrogen donated by the additives reacts with the free radicals that are formed during the carbonisation process and helps to stabilise the reactive radicals, preventing the formation of a semi-coke at too early a stage in the process (Machnikowka *et al*., 2002). Thus, the additives increase the fluidity of the system because they stop the free radicals from bonding with the other carbons (Figure 2.8).

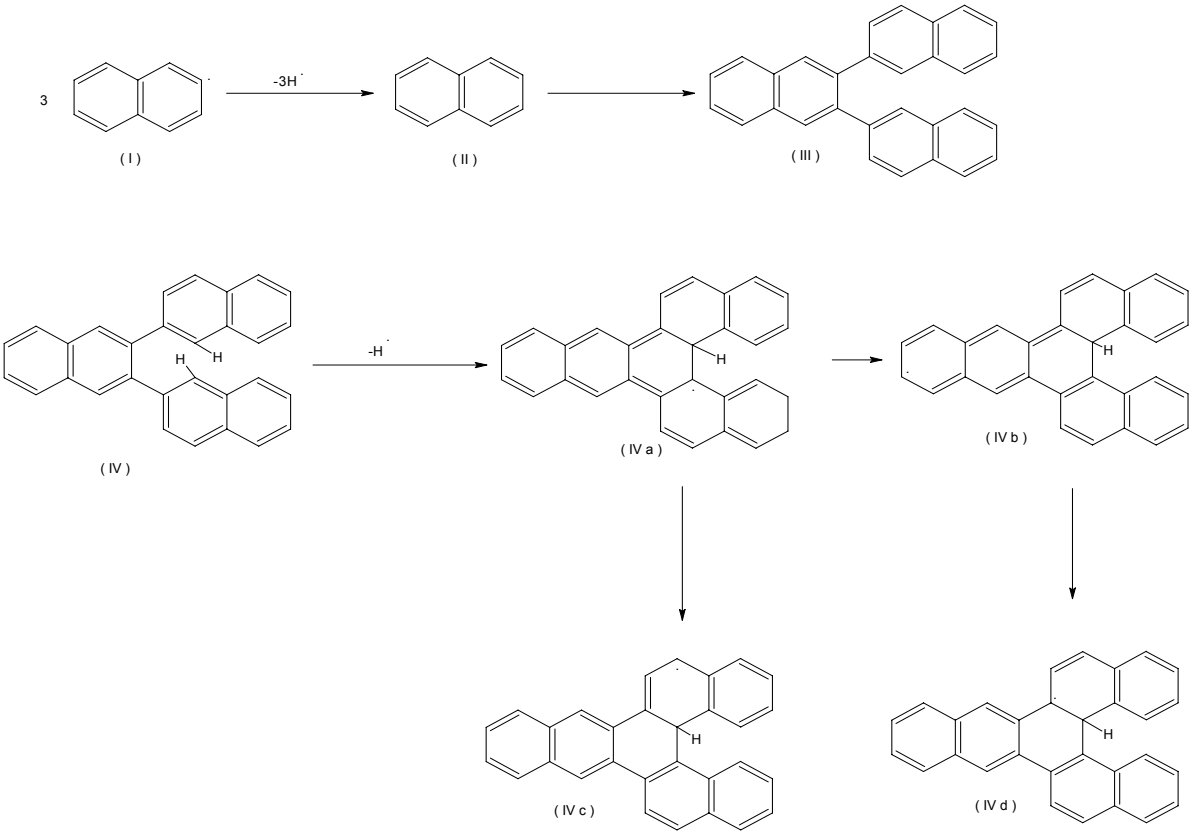

Figure 2.8: Formation of stable odd-alternate free-radical structures during carbonisation

(Lewis and Singer, 1993)

Figure 2.9 shows the gradual transition of the mesophase upon heating into graphite and Figure 2.10 shows the effect of hydrogen stabilisation on the carbonisation process.

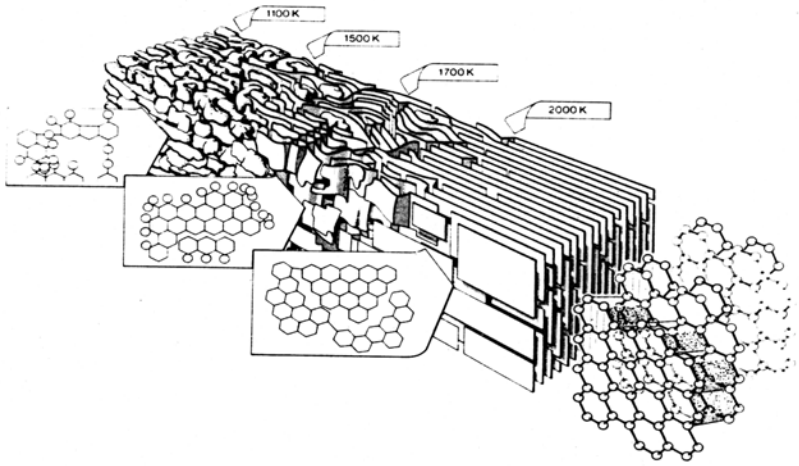

Figure 2.9: **Change in structure of non-graphitic mesophase conversion to graphitisable carbon**

(Marsh H, 1989)

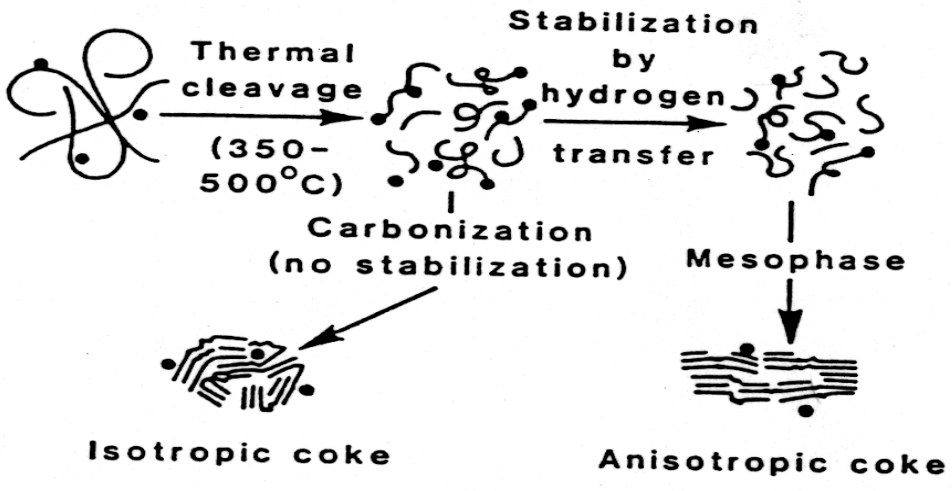

Figure 2.10: **Influence of hydrogen transfer reactions during pyrolysis of petroleum residues on carbon formation**

(Marsh H, 1989)

However, not all mesophases have the same viscosities: if the viscosity is too high, the mesophases that form never mix together but rather form a mosaic structure, which ultimately forms the isotropic carbon that produces the shot cokes. As the viscosity increases, the fluidity decreases and the mesophase formation is reduced. Even a mesophase with the lowest viscosity may form isotropic carbon. The coalescence of the mesophase is very sensitive to the presence of insoluble material, this is known as 'quinoline insoluble' (QI) (Delhaès, 1979). Coal-tar pitches can contain 12 wt % QI, which could result in a very polycrystalline coke Machnikowaka *et al*, 2002).

2.8.1 Isotropic carbons

Isotropic carbons are known as non-graphitisable carbons. They are formed from the materials that do not fuse or melt during the carbonisation process. These materials are often wood, non-fusing coal such as lignites, and anthracite nuts and nutshells, and most of the biomass material. Isotropic carbons can be prepared from the polymeric precursors that are initially heavily cross-linked or are developing cross-linkages in the early stages of carbonisation.

During the early carbonisation stages the bonds within the macromolecular system (polymer) break to give radicals. Above the heat-treatment temperature of 500 ºC there is a rapid increase in the concentration of free radicals. These early stages involve the elimination of small molecules, such as volatile material in the form of water, methanol, methane and carbon dioxide. Such eliminations create space within the polymer and at the same time radicals are generated at surfaces, either combined with each other or with abstract hydrogen from the system (Marsh, 1989). The process begins at a temperature of 350 ºC under nitrogen. Aliphatic side-chains are linked to the forming aromatic domain by mixed ketonic and ether linkages. The carbonisation process is the simultaneous process of eliminating small molecules and rearranging the carbon atoms (radicals) in order to form more stable layers of six-membered carbon rings, albeit imperfectly. At about 550 ºC all of the aliphatic carbon is converted to aromatic C-H. (Marsh, 2002).

2.8.2 Anisotropic carbons

Anisotropic carbons are graphitisable carbons. Graphitisable carbons are produced from coal-tar pitch and petroleum pitch (Brooks and Taylor, 1968). These materials are a complex mixture of polynuclear hydrocarbon systems with functionalities and would appear to be very good starting materials for graphitisable carbons (Marsh, 2002).

2.9 HYDROGEN TRANSFER DURING CARBONISATION

Graphitisable carbons are formed from the starting material, such as coal-tar and petroleum pitches, going through a fluid stage (mesophase) during carbonisation. This fluid phase is required to produce graphitisable carbon. After the formation of the anisotropic mesophase spheres, the growth and coalescence of the spheres produces anisotropic carbon material (Brooks and Taylor, 1965). This leads to intermolecular hydrogen-transfer reactions. The availability of transferable hydrogen in terms of the stabilisation of reactive free radicals in mesophase development is a crucial factor in the formation of graphitisable carbons (Swietlik *et al*., 2002).

During the carbonisation process the precursor starts to give off free radicals because of the thermal cleavage of the C-C and C-H bonds in the reactive component (Díez *et al.,* 1999). When these thermally reduced radicals are not stabilised by transferable hydrogen from the system, they may form isotropic carbon and small-sized anisotropic carbon structures by recombining with the other species present in the highly viscous system. The growth of aromatic molecules occurs as the radicals are stabilised by the hydrogen-transfer reaction, and also the growth and coalescence of mesophase takes place under conditions of low viscosity or high fluidity with the result that more ordered anisotropic carbon is formed.

The amount of transferable hydrogen is related to the hydrogen donor and acceptor abilities. Hydrogen donor ability is strongly influenced by the hydro-aromatic structures because they cause the hydrogen radicals to stabilise thermally induced radicals in order to raise species with low molecular weight and improve the fluidity of the reaction system. This fluidity allows the carbon planes in the network to stack

parallel to each other and form the more ordered optical texture of the resultant carbon material.

Pitch displays a dual nature in terms of hydrogen-transfer ability because of its compositional complexity. In the presence of a hydrogen acceptor compound it behaves as a hydrogen donor, but when treated with a hydrogen donor agent it becomes a hydrogen acceptor. The hydrogen donor ability of pitch is primarily attributed to the presence of compounds with hydro-aromatic and naphthenic rings, although the methylene and ethylene bridges linking two aromatic rings can be a source of transferable hydrogen (Honda, 1998). Since they have primary hydrogen acceptor ability, thermally induced reactive free radicals and oxygenated functional groups must be taken into account. This transferable hydrogen reacts with aromatic carbon atoms with high energy density.

The hydrogen acceptor properties of hetero-aromatic and hetero-substituted compounds depend on their reactivity under reaction conditions. Ketones, quinones and some ethers are readily hydrogenated, in contrast to phenols, carboxylic acids and furan, pyrrol and pyridine derivatives which are inactive. The unsubstituted aromatic compounds show different hydrogen acceptor abilities. Most of the acenaphthylene compounds accept hydrogen readily due to the presence of an olefin bond (Díez *et al*., 1999).

The amount of hydrogen transferred from coal to hydrocarbons can decrease in the range of naphthalene > anthracene > pyrene. Naphthalene abstracts hydrogen from methylene bridges that have lower activity than anthracene (Díez *et al.*, 1999). Insoluble pyridine shows the lowest values for both hydrogen donor and acceptor abilities, whereas soluble hexane freed from polar compounds shows the highest hydrogen donor ability.

2.10 COMMERCIAL COKING PROCESS

The main aim of coking is to convert vacuum distillate residue into naphtha and gas oil, but coke is also produced. There are different coking processes, which include delayed coking and fluid coking.

2.10.1 Delayed coking process

Delayed coking is a thermal cracking process, which increases the molecular aggregation in petroleum-based residues or coal-tar pitches, leading to extended mesophase domains. This is a semi-continuous operation in that the feed is introduced continuously but the coke is recovered intermittently. This coking process involves several reactions, such as dehydrogenation, rearrangement and polymerisation. Polynuclear aromatics have six carbon aromatic rings concentrated from aromatic oils, such as decant oil and pyrolysis residue. The vacuum residues contain asphaltic compounds, which are mostly heterocyclic molecules.

This coking process is attractive because it has the ability to produce coke with controllable microstructures. It is performed in a coking drum and is designed to give the final product of delayed coke. Delayed coke displays, with only a few exceptions, better graphitisability than cokes produced by other coking processes, even if the same feedstock is used. Delayed coke contains a mass fraction of volatile matter between 4 and 15 wt %, which can be released during heat treatment. Pure petroleum feedstocks have a large number of cross-linkages with fewer than six carbon atoms.

2.10.1.1 Products from delayed coking

This process produces desirable liquid products (naphtha and gas oil) and by-products (coker gas and solid coke). Naphtha from coking units has a high olefin content and is usually sent to the hydrotreating units in the refinery for stabilisation. Gas oil is produced as a heavy liquid and is sent to the catalytic cracking units where the valuable fuels (gasoline, diesel and jet fuel) are produced. Coker gas goes to the gas plant where sulphur is removed and the lighter end can be used as fuel gas in the refinery. Solid coke is the only finished product in the delayed coking process. Cokes produced from the delayed coking process are needle, sponge and shot coke.

Needle coke is an end-product of the delayed coking process. It has needle-like appearance and a microscopic extended crystalline structure. Needle coke is generally produced from the highly aromatic residues from the steam cracking of gas oil. Its appearance and the orientation of the graphene layers is a consequence of

the evolved gaseous products percolating through the mesophase, which must not have too high a viscosity (Mochida *et al*., 1996). Close control over the temperature, time and feedstock is essential. Needle cokes are used for making graphite electrodes for electric-arc furnaces.

Delayed coking feedstock tends to produce isotropic or amorphous cokes and when their porosity is very visible, they are called *sponge coke* and are used for the production of carbon anodes, which are applied in the production of aluminum. The sponge coke exists in two states, *calcined* and *green*. Calcined sponge coke is used in aluminum anodes, TiO_2 pigments and carbon raisers. Green coke contains about 10 – 15% volatile substances and is sent to a rotary calciner at 1 200 ºC to remove the volatiles. This green coke is used in silicon carbides, foundries and coke ovens (Rodríguez-Reinoso *et al*., 1998).

Shot coke is an abnormal coke resembling small balls and is produced during fluidisation in the coke drum. It is more isotropic in texture and is hard with a low porosity and high density, which makes it difficult to crush. Most sponge cokes are used as fuel, but those with a low sulphur and metal content can be used in aluminum production. This type of coke is also in a green state.

2.10.2 Fluid coking process

This method was developed by EXXON in 1954. It is a continuous process in which heated coker feeds are sprayed into a fluidised bed of hot coke particles, which are maintained at 20 – 40 psi and 500 ºC. The feed vapours are cracked while forming a liquid film on the coke particles. The particles grow by layers until they are removed and new seed coke particles are added. Coke for the aluminium industry is calcined to less than 0.5% volatiles at 1 300 to 1 400 ºC before it is used to make anodes.

This process is used only to produce lower-grade fuel coke. Unlike the delayed coking process, this is a continuous process in which the coke is removed and quenched on a continuous basis. Lower yields are obtained because of the higher temperatures and more severe cracking.

2.11 KINETICS OF CARBONISATION

The kinetics of carbonisation has been studied by thermogravimetric, thermovolumetric and differential thermal analysis (DTA) techniques (Pitt and Millward, 1979). With the help of plasticity and dilatometric measurements, the mathematical model of the reactions leading to the transformation of coal into coke has been postulated as:

(1) Coking coal $\xrightarrow{K_1}$ metaplast

(2) Metaplast $\xrightarrow{K_2}$ semi-coke + primary volatiles

(3) Semi-coke $\xrightarrow{K_3}$ coke + secondary gas

Where K_1, K_2 and K_3 represent the relevant velocity constants (Gibson and Gregory, 2000).

Reaction 1 is a depolymerisation reaction in which coal is transformed into the unstable intermediates responsible for the plastic behaviour.

Reaction 2 represents the transformation of the metaplast into semi-coke (resolidification), which is accompanied by the evolution of gas, causing the mass to swell.

Reaction 3 represents the semi-coke, in which case units of methane and hydrogen are lost to give a more compact and coherent coke.

2.12 GRAPHITISATION

Graphitisation is a solid-state transformation of thermodynamically unstable non-graphitic carbons into graphite by thermal activation. The degree of graphitisation depends on the temperature of the heat treatment and the time to graphitise.

Non-graphitised carbons are substances consisting mainly of the element carbon with two-dimensional long-range order of the carbon atoms in a planar hexagonal network, but without any measurable crystallographic order in the third direction, called the *c-direction,* apart from more or less parallel stacking.

Innumerable non-graphitic carbons can be converted into graphitic carbons by heat treatment above 2 220 ºC. This conversion is simply called *graphitisation*.

2.12.1 Graphitisable and non-graphitisable carbons

The graphitisable carbons (Figure 2.11) pass through a fluid stage during carbonisation, thereby allowing large molecules of aromatic compounds to align with each other by forming the mesophase precursor of the graphitic structure, which is important for the development of coke.

Non-graphitisable carbons (Figure 2.12 and 2.13) are those that cannot be transformed into graphitic carbon solely by heat treatment up to 3 300 K under atmospheric or lower pressure, whereas graphitised carbons can be converted to graphitic carbons by heat treatment under atmospheric pressure and temperature.

Non-graphitisable carbons are formed from wood, nutshells and non-fusing coals. The macromolecular (polymeric) structure of these materials remains the same during heat treatment, only losing small molecules by degradation and forming more cross-linkages by preventing the fusion from taking place.

Figure 2.11: Graphitisable carbon/coke

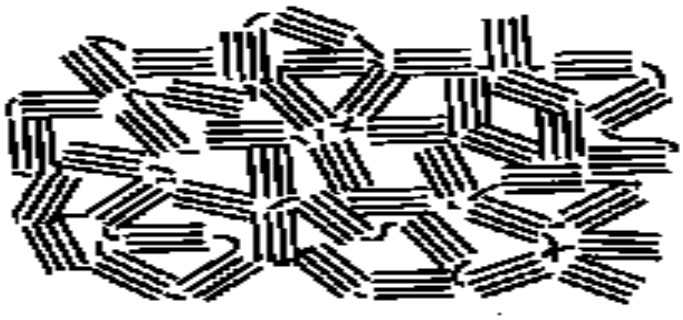

Figure 2.12: Non-graphitisable carbon/coke

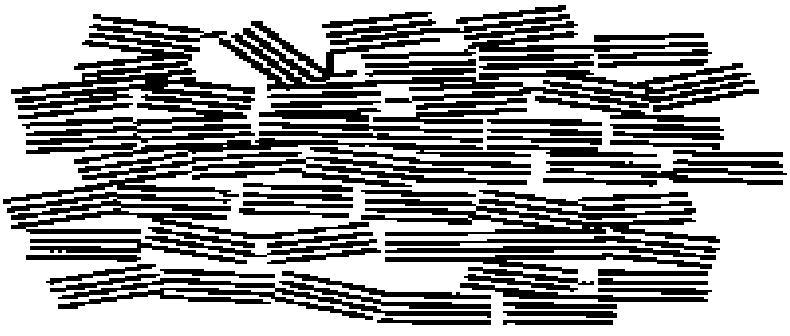

Figure 2.13: Partially graphitisable carbon/coke
(Bundy *et al.*, 1996; Marsh, 2002)

2.13 EXPERIMENTAL TECHNIQUES

2.13.1 Diffuse reflectance infrared Fourier transform spectroscopy

Diffuse reflectance infrared Fourier transform (DRIFT) spectroscopy was evaluated as a method for the determination of volatile matter, fixed carbon, ash, heating value, carbon, hydrogen, nitrogen, total sulphur and maximum vitrinite reflectance (Carlos *et al.*, 1996).

Spectroscopic techniques, such as DRIFT spectroscopy, capable of rapid non-destructive analysis with little sample preparation are of great interest for coal analysis. However, coal (and related carbonaceous materials such as activated carbon and carbon black) strongly disperses infrared radiation, thus reducing the energy that reaches the detector. The infrared radiation of coal has a low noise signal, poorly defined baselines and broad, overlapping bands. There is also little qualitative variation amongst the spectra of different coals, even the different ranks. Finally, great care must be taken to ensure that the coal sample used in DRIFT (a few milligrams) represents the macroscopic sample under evaluation.

2.13.2 Non-isothermal themogravimetric analysis

Themogravimetric analysis (TGA) monitors the weight losses as the temperature is increased. Weight losses occur as a result of the driving-off of water and other volatiles. At higher temperatures, there is degradation of the products formed. The technique can be used both to examine the state of the material (i.e. for the presence and quantity of volatiles) and to investigate the process of degradation. The method identifies the temperatures at which significant changes occur. Control of the atmosphere and/or analysis of the products evolved give information about the chemistry of the degradation process. In cases where the various weight losses are not completely discrete, use of the derivative curve is recommended.

Mettler TGA/SDTA 851^{e}: This thermogravimetric analyser is equipped with an additional sensor to record the temperature difference between the temperature measured directly at the sample and the model's reference temperature. This measuring signal is called SDTA (signal DTA) and it indicates, for example, whether

a transition is exothermic or endothermic, analogous to differential scanning calorimetry (DSC).

2.13.3 Nuclear magnetic resonance spectroscopy

Nuclear magnetic resonance spectroscopy (NMR) is an analytical tool that is very valuable in organic chemistry as it gives essential information on the C-H framework in an organic compound. The proton gives bands corresponding to aliphatic protons and carbons (Khan *et al.*, 2003). It makes provision for the rapid and non-destructive determination of the total hydrogen content and for the distribution of hydrogen among chemical functional groups in the sample.

NMR is based on the measurement of the absorption of electromagnetic radiation in the radio-frequency region roughly between 4 and 900 MHz. In order to cause nuclei to develop the energy state required for absorption to occur, it is necessary to place the analyte in an intense magnetic field (Skoog and Holler, 1992).

A nuclear magnetic resonance spectrometer is essentially a radio receiver, which in addition has a transmitter, a magnet and a minicomputer connected directly to it. In modern NMR instruments these basic components are closely integrated, to an extent depending on the year of manufacture, the maker and the specific purpose.

2.13.4 Raman spectroscopy

Raman microscopy is a non-destructive technique, very appropriate for studying at the micrometre scale the chemical bonding, the phase composition and the crystalline state of solids, from poorly organised to well-crystallised structures. This technique is based on the analysis of the spectral characteristics of the vibrational modes associated with the Raman peaks (wave number, bandwidth and intensity) (Urban *et al*., 2003).

Raman microscopy has been widely applied to the study of carbon materials and their graphitisation behaviour at high temperature. The hexagonal graphite structure (space group D^4_{6h}) is characterised by two Raman active vibrational modes with E_{2g} symmetry (E_{2g1} and E_{2g2}). Both modes correspond to in-plane vibrations of carbon

atoms. Whereas the former mode corresponds to shear displacement of whole graphene layers (νE_{2g1} = 42 cm^{-1}, not considered here), the latter involves the stretching of the sp^2 C-C bond. Owing to the C-C covalent bond (as compared with weak interlayer bonding), the E_{2g2} mode (commonly referred to as the G band) is characterised by a much higher frequency (νE_{2g2} = 1 582 cm^{-1}) (Cottinet *et al.*, 1988).

In the case of disordered carbons (e.g. turbostratic carbons), the Raman spectra commonly show an additional feature at about 1 350 cm^{-1} (D band or A_{1g} mode), as well as, in some cases, another weak band at around 1 620 cm-1 (D' band), close to the G band. Both the D and D' bands are generally associated with a broadening of the G band (Veres *et al.*, 2004). They are assigned to defects within the carbon microtextures (edges, distorted graphene layers, etc.) in relation to the ideal graphite structure .The 1 350 cm^{-1} bands are attributed to the finite crystal size. The intensity ratio of the 1 350 cm^{-1} band to the 1 580 cm^{-1} band can be used to measure the crystal size L_a of the graphite sheet (Montes-Morán *et al.*, 2002).

2.13.5 X-ray diffraction

X-ray diffraction (XRD) is a useful analytical technique for determining the changes in structure that occur during graphitisation. As with all crystalline materials, a sharp diffraction pattern is obtained with single-crystal graphite. Pronounced crystallinity is indicated by the development of the 002, 004 and 101 peaks (Chunlan *et al*, 2004). The crystal size is measured by X-ray diffraction from the breadth of the (110) and (002) lines. The interlayer spacing (d_{002}) is also determined from X-ray measurements and is another indication of the degree of graphitisation (Marsh, 2000).

2.13.6 Optical microscopy

In order to view samples under an optical microscope, it is necessary to prepare a highly reflecting polished surface. To facilitate the polishing of very brittle samples, a cross-section of each sample is mounted in a Bakelite resin. In order to expose the sample and prepare a flat surface, the initial grinding is carried out on grinding disc fitted with 120, 600 and 1200 grades of diamond disc, over which water flows

continuously. Grinding is carried out with the successive grades of disc until a flat even surface is obtained, ready for polishing.

Polishing is then carried out using successive grades of diamond pastes (9, 6 3 and 1 microns), starting with the coarsest and finishing with the very fine gamma. A rotating lap is used for the “slow-outing” 150 grades, whilst a stationary lap is used for the final polishing using the diamond paste (Chaudhuri *et al*, 2005). The laps are covered with cloth (Poly Pan2) and water is continuously dripped onto the cloth. The sample can then be analysed under an optical microscope.

CHAPTER 3: EXPERIMENTAL

3.1 COAL SOLVENT EXTRACTION

The coal used for this study is from Tshikondeni mine in Venda, Limpopo Province. The coal was dissolved in a mixture of dimethylformamide (DMF) and sodium hydroxide, using the procedure reported by Morgan (2000). To a 3 ℓ reactor with a hot oil jacket and operated at temperature of 90 to 94 °C, 240 g of coal was added, together with 2 400 g of DMF (see Figure 3.1). When the temperature had reached 94 °C, then 24g of sodium hydroxide (CP) in pearl form was added. A slow stream of nitrogen was flushed into the reaction mixture in the reactor to prevent oxidation.

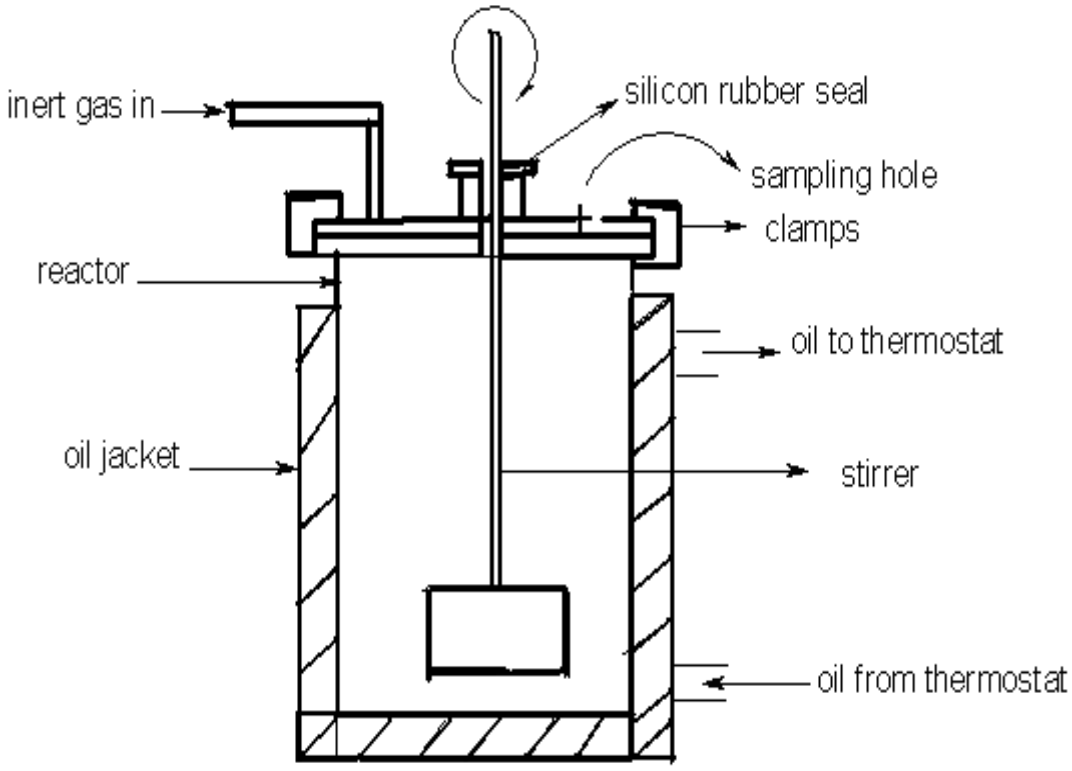

Figure 3.1: Three litre reactor used for coal extraction

During extraction, the progress was monitored as follows: samples of the slurry were taken from the reactor at suitable time intervals. The samples were centrifuged for 6 minutes at 3 000 r/min using a Clements centrifuge. About 0.1 g of supernatant

solution was weighed accurately into a 50 ml volumetric flask and made up to the mark with DMF. The optical absorbance was measured in a spectrophotometer at 600 nm.

The measured absorbance was then corrected to a 0.1 g sample. The extraction period was 3 to 6 hours with 3 ℓ reactor. The mixture of Refcoal solution and the inorganic components, together with the undissolved organic components of the coal, was transferred into a centrifuge bottle. The mixture was centrifuged at room temperature at 4 300 r/min for 1 hour, using a Beckman GPR centrifuge. The Refcoal solution (supernatant) was separated from the residue by decantation.

Distilled water was used to precipitate the Refcoal solution into a centrifuge bottle. The mixture of Refcoal solution and distilled water was then centrifuged for 30 minutes at room temperature at 4 300 r/min. Thereafter the supernatant solution was replaced by distilled water and the Refcoal mixture was re-suspended in the water by shaking the mixture for 3 minutes. The resulting Refcoal gel was washed four times with fresh distilled water by re-suspending it in water, followed by centrifugation at 4 300 r/min. The crude product was dried in an oven at about 60 °C for 24 hours.

3.2 OXIDATION OF REFCOAL SOLUTION

The gas burette shown in Figure 3.2 was used to oxidise the Refcoal solution.

Refcoal solution (200 ml before washing) was put in a three-necked round-bottom flask equipped with two rubber septa on the side of the necks. The water burette has a maximum capacity of 2 ℓ of oxygen gas. The neck on the one side of the reaction flask was connected to atmospheric pressure for oxidation, while the centre neck was connected to a stirring rod, shown in Figure 3.2, although stirring was not done immediately. Stopcock 2 and the gas burette stopcock were opened to the atmosphere before the hose from the oxygen tank was connected.

The gas burette was filled with water up to the level of the stopcock by raising the levelling bulb, and the gas burette stopcock was closed. The vacuum hose and the hydrogen tank hose were attached to stopcock 2. The system was opened to

vacuum by turning stopcock 2. The solution in the reaction flask bubbled as the flask was evacuated. Stopcock 2 was turned again to fill the system with oxygen gas. This procedure was repeated three times.

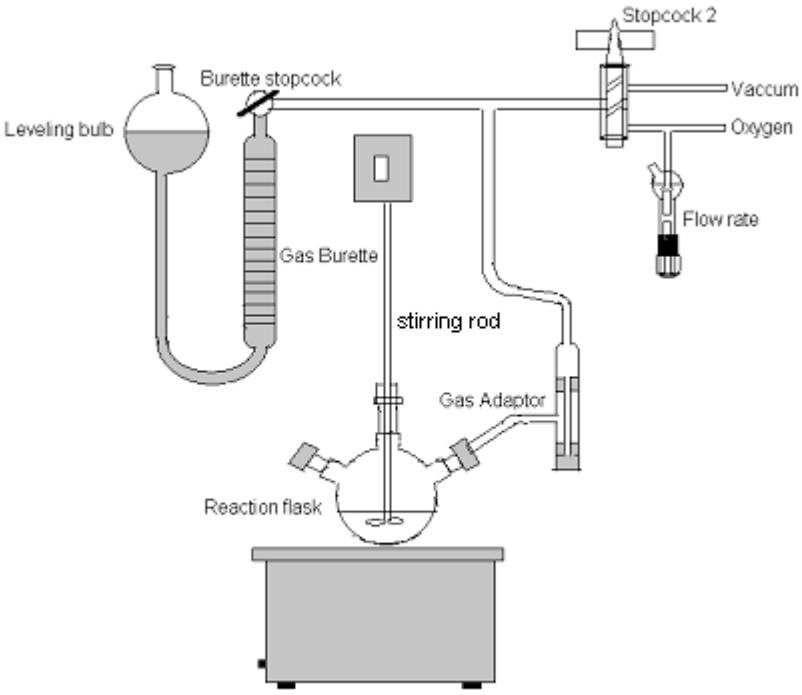

Figure 3.2: Gas burette used for Refcoal oxidation

The levelling bulb was detached from the ring stand and lowered below the level of the water in the burette. The burette stopcock was then opened and lowering of the levelling bulb was continued to fill the oxygen burette with the appropriate amount of gas. The initial water level in the burette was recorded as zero. Stopcock 2 was then closed, but the burette stopcock was left open and stirring was begun. The levelling bulb was reattached at an elevated position on the ring stand. The vacuum hose and the oxygen tank were disconnected.

The amount of oxygen consumed was monitored by reading the burette volume every 3 minutes (see Figure 3.3 below). By raising and lowering the levelling bulb until the water level is the same in both, the bulb and the burette can read the burette volume. At least about one-third of the gas was consumed in the first 20 minutes. When the reaction was complete, the Refcoal solution was saturated with oxygen. The saturated solution was removed from the reaction flask by rinsing it with distilled water.

3.3 PREPARATION OF DIABIETIC ACID

The apparatus set-up as illustrated in Figure 3.3 was used for the dimerisation of abietic acid, the mechanism of which is shown in Figure 3.4. A Roto-vapor was used to remove the solvent. Figure 3.5 illustrates the Roto-vapor apparatus.

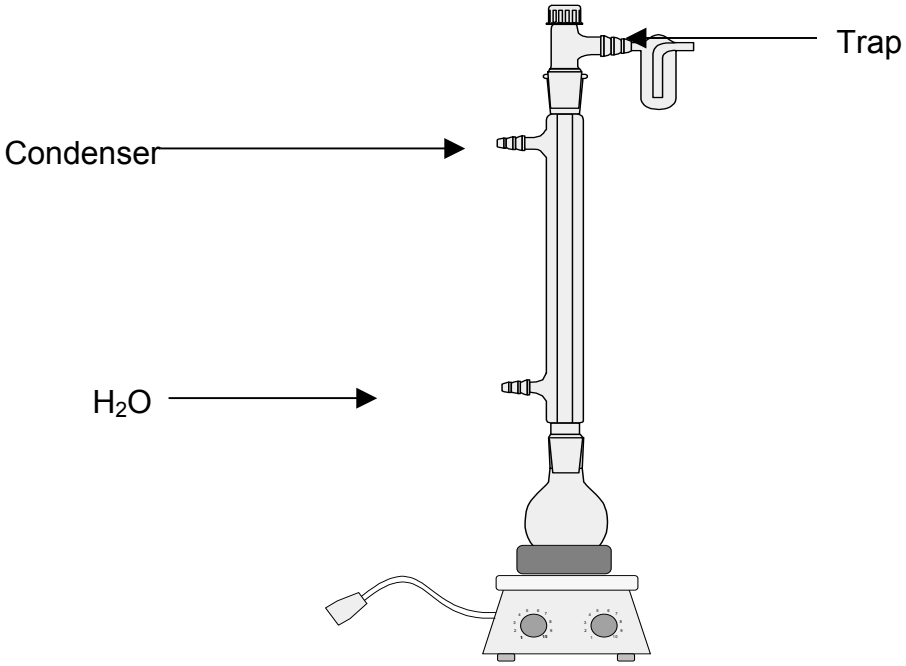

Figure 3.3: Apparatus used for the dimerisation of abietic acid

About 10.3 g of abietic acid supplied by Aldrich was dissolved into 100 ml of chloroform, and 3 ml of concentrated sulphuric acid (98%) was added drop-wise. The reaction flask was warmed at 45 ^{o}C in a water bath, and the heating and stirring continued for 5 hours (Sinclair *et al*, 1970). The product was then washed four times with distilled water.

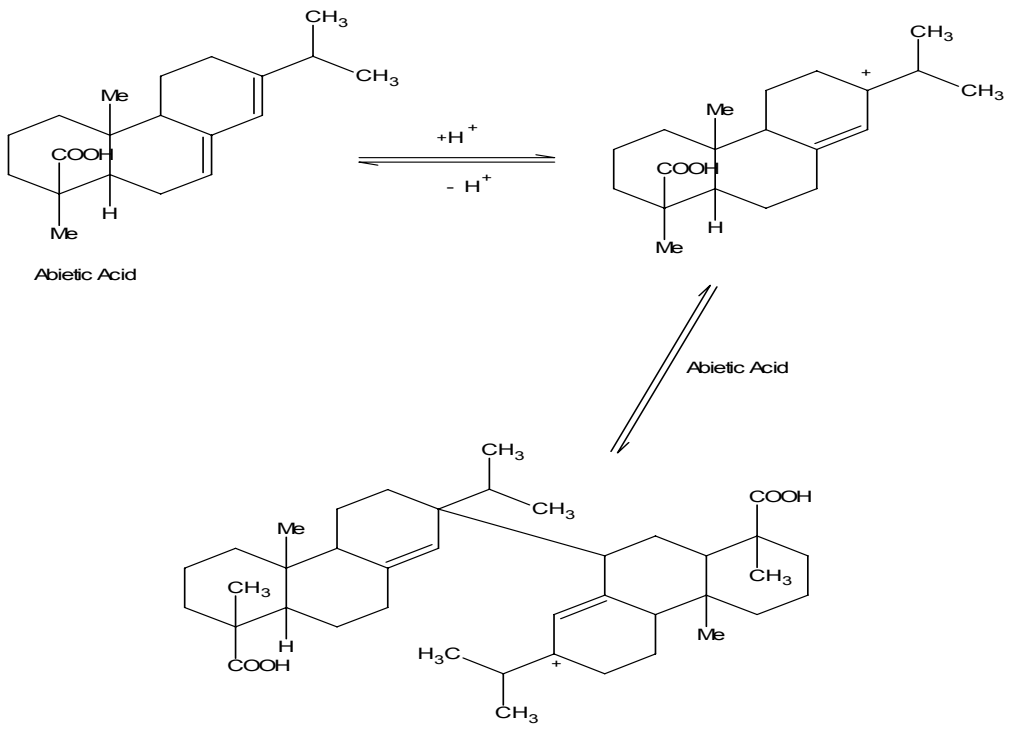

Figure 3.4: Mechanistic pathway accounting for the first step in dimerisation, and by-products occurring during the acid treatment of abietic acid

The washed product yielded a dark yellow-brown solution which was then washed again with saturated sodium chloride solution until the aqueous wash was neutral. The chloroform layer was separated and evaporated in the Roto-vapor. The product obtained was dried in an oven at 60 °C for 16 hours. The dried final product was analysed by NMR spectroscopy.

Diabietic acid was then used as an additive during carbonisation of oxidised Refcoal. After oxidation, the oxidised Refcoal solution prepared as described in Section 3.2 was mixed with different percentages (3,5 and 10%) of diabietic acid. This solution was washed four times using distilled water and then centrifuged for 30 minutes at room temperature at 4 300 r/min. The product was dried in an oven at 60 °C for 24 hours.

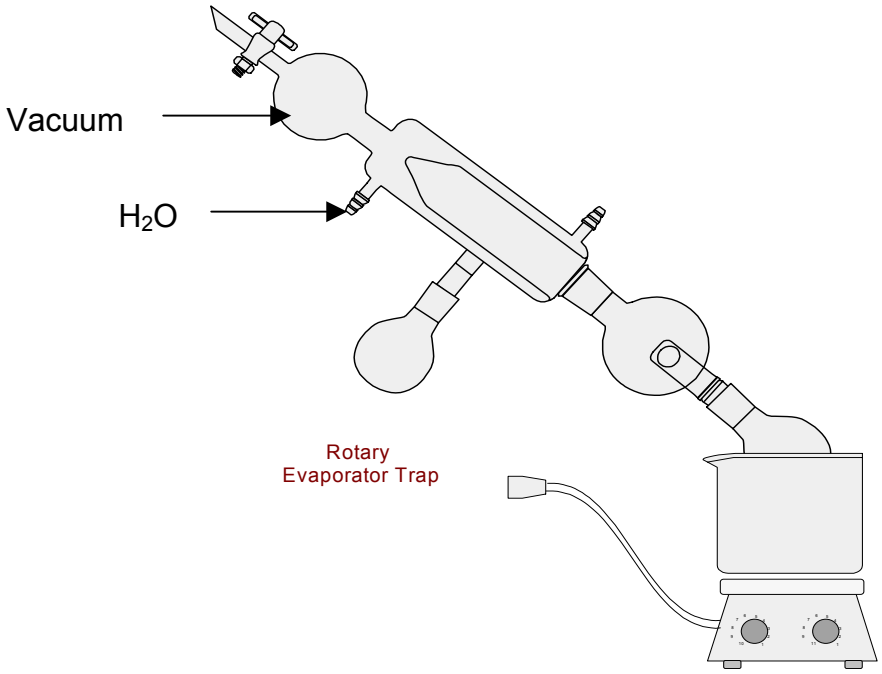

Figure 3.5: Roto-vapor apparatus used to remove solvent

3.4 CARBONISATION OF THE SAMPLES

Refcoal prepared as described in Section 3.1 was carbonised as follows:

About 0.5 – 1 g of dry oxidised Refcoal was ground with diabietic acid into fine particles and weighed in glass capillary tubes (diameter 3 mm and height 180 mm). The tubes (with the samples) were closed by melting the glass at the end and placed inside a metal tube 'bomb'. The tube bomb was then placed in a vertical coking furnace (Mochida *et al*, 1986).

The samples in the tubes were heated from room temperature to 400 °C at a heating rate of 10 ºC/min and left at 400 ºC for 1 hour, after which the temperature was increased to 680 °C and held there for 2 hours. If the temperature is too high (higher than 680 ºC), it causes the glass to soften and the elevated pressure causes the tubes to expand. Some of the tubes broke in this way, making it impossible to separate the glass and the cokes. All the rest of the samples were heated to 680 ºC only.

After heat treatment, the soaked samples were allowed to cool to room temperature. The tubes were then removed from the furnace. The glass capillary tubes were opened and the samples were dissolved in hydrofluoric acid (HF) for 2 days. Thereafter the cokes were filtered, and then washed with distilled water until all the acid had been removed. The texture of the filtered cokes was examined by thermogravimetric analysis (TGA), Raman spectroscopy X-ray diffraction and optical microscopy.

3.5 SAMPLE ANALYSIS

3.5.1 Diffuse reflectance infrared Fourier transform spectroscopy

The Refcoal and oxidised Refcoal samples were mixed in potassium bromide (KBr) in a ratio of 1:20. The instrument used for sample analysis was a Perkin-Elmer Spectrum GX FTIR spectrometer (Norwalk, CT, USA), with a room-temperature deuterated triglycine sulphate (DTGS) detector. A DRIFT sampling accessory was used. All the spectra were collected from 13 scans at a resolution of 8 cm^{-1} and a gain of 1.0 over the frequency range 4 000 to 600 cm^{-1}. The spectra were rated against the background air spectrum.

3.5.2 Nuclear magnetic resonance

The instrument used for NMR analysis was Bruker AM 300 spectrometer. ^{1}H NMR spectra of Abietic acid and Diabietic acid were obtained from $CDCl_3$ solution in a 5mm tube using the high-resolution probe. $CDCl_3$ solution was prepared by dissolving 0.01g of sample (Abietic acid/ Diabietic acid) in 0.5ml of solvent, which is Chloroform.

3.5.3 X-ray diffraction

A series of about 2.0 g of carbonised samples were ground together with about 0.13 to 0.2 g of silicon (99.9% pure supplied by MERCK laboratories, with crystallite sizes up to 43 µm (430 000 Å) to pass through a 240 B.S.S. mesh sieve. About 0.6 g (16 drops) of PEG and 1 to 2 ml of ethanol as a wetting agent were added and the mixed in. After thorough mixing, the ethanol was evaporated. The ground sample was placed in a 0.3 mm silica glass capillary and an X-ray powder photograph was

taken using a 37.4 mm camera fitted to a Phillips PW 1010/30 X-ray diffraction unit operating with filtered Co radiation.

3.5.4 Optical microscopy

Samples of the cokes (carbonised) produced were examined under polarised light in an optical microscope. The samples where polished as decribed earler under experimental techniques section 2.13. After being polished, the coke samples were mounted on glass slides with plasticine using a hand mounting press (Struers) to enhance evenness, the polishing surface being protected during the mounting by a lens tissue. The samples were then placed on the rotating stage of the microscope (Standard Universal-Carl Zeiss) and examined by reflected polarised under an oil-immersion Antiflex-epi Zeiss objective lens. The results were photographed onto 33 mm slides. For each sample a set of two measurements was taken: the object stage was turned through an angle of 90^{o} and the maximum and minimum reflectance values recorded.

3.5.5 Non-isothermal themogravimetric analysis

The analyses of the carbonised samples were carried out in Mettler Toledo TGA/SDTA 831^{e} thermal analyser. About 10 mg of each sample was placed in a 70 μl capacity alumina crucible. The samples were heated in a thermo balance up to 1 000 ºC, at a rate of 10 ºC min^{-1}, under nitrogen flow of 30 ml/min.

3.5.6 Raman spectroscopy

Raman spectroscopy was used to analyse the carbonised samples. The Raman spectra were recorded with an XY Raman spectrometer from Dilor®, using the λ = 14.3 nm laser line of a Coherent Innova®90 Ar^{+}-laser, with a resolution of at least 2 cm^{-1}.

The samples were recorded in a backscattering configuration under the microscope attached to the instrument, using a 30-x objective. A liquid-nitrogen-cooled CCD detector was used with the laser power at 100 mW at the laser exit, resulting in a laser power of < 20 mW at the sample. The spectra were baseline-corrected, using the Labspec software program supplied by Dilor®.

CHAPTER 4: RESULTS AND DISCUSSION

4.1 EXTRACTION OF THE COAL

The raw extraction data are reported in Table A.6 of the Appendix. Figure 4.1 gives the results obtained for duplicate runs. It shows the course of coal extraction expressed as absorbance (optical density) versus time. The notable feature is that the solvent-alkali extraction process exhibits an induction period during which the rate of dissolution is slow. For the present reaction conditions the induction period is about 1 hour. The induction period is followed by a rapid dissolution stage before a plateau value in the absorbance is reached. It is assumed that the coal extraction is complete when this plateau value (of about A = 1,1 at 600 nm) has been reached. At this point the solids content of the solution was about 8% (mass per mass).

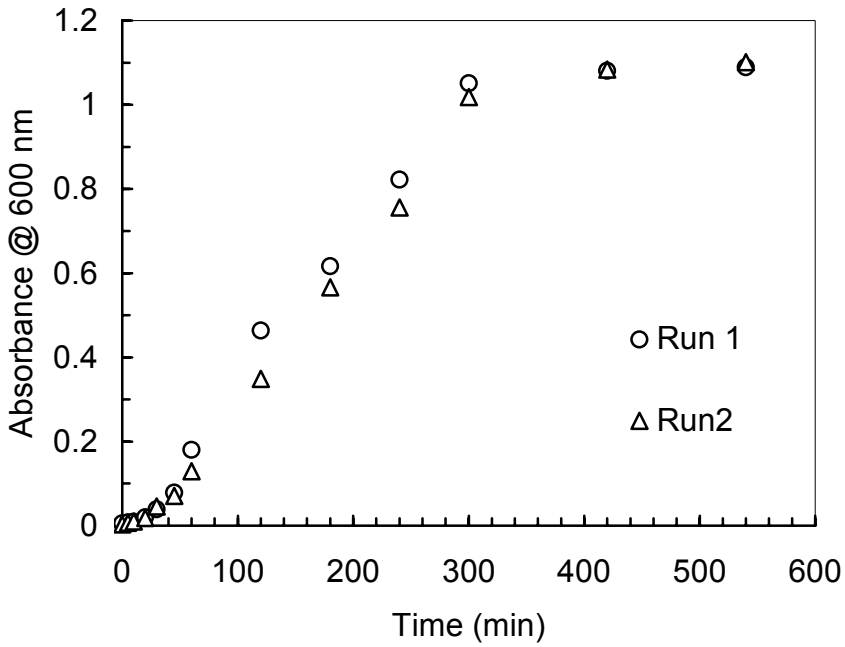

Figure 4.1: Progress of extraction of coal at 94 °C
Reagent ratios were DMF:coal:NaOH = 100:10:1

4.2 THE OXIDATION OF REFCOAL

The raw Refcoal oxidation data is reported in the Appendix, Table A.7. The oxygen consumption was monitored using the gas burette apparatus shown in Figure 3.2. The results of a typical run are shown in Figure 4.2. There was a definite endpoint beyond which oxygen absorption ceased. Figure 4.2 shows that for the first 15 minutes, the volume of oxygen increases rapidly until about 300 ml has reacted. During this process the solution becomes more viscous and also warmer as a result of the exothermic oxidation reaction. After oxidation the solids were recovered in the usual way and analysed by diffuse reflectance infrared Fourier transform (DRIFT) spectroscopy.

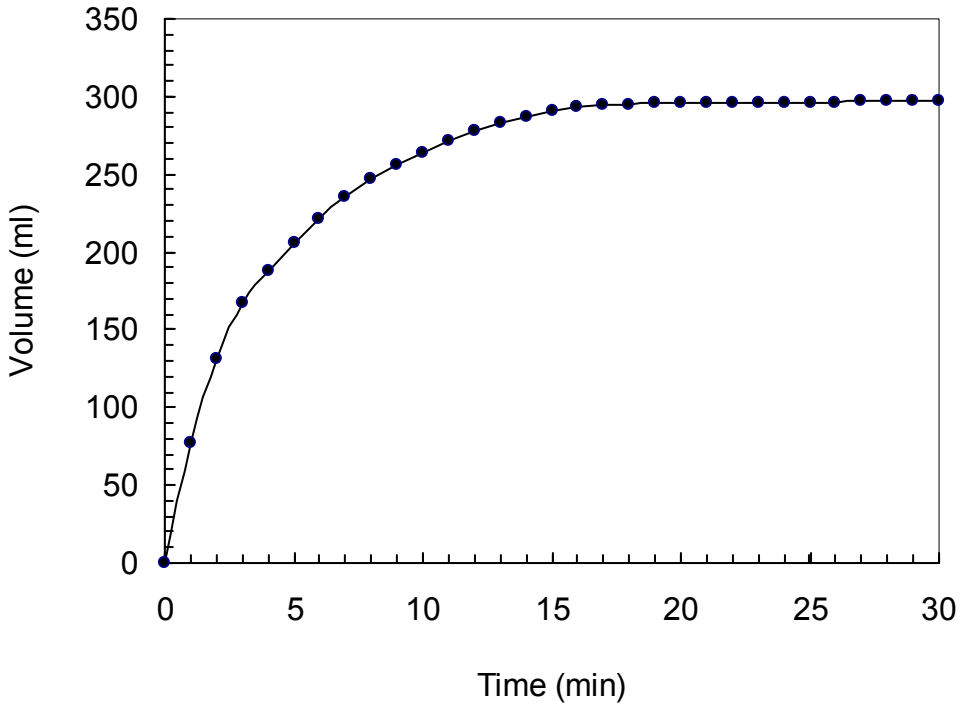

Figure 4.2: Volume of oxygen consumed on treating 200 ml of Refcoal solution at ambient temperature

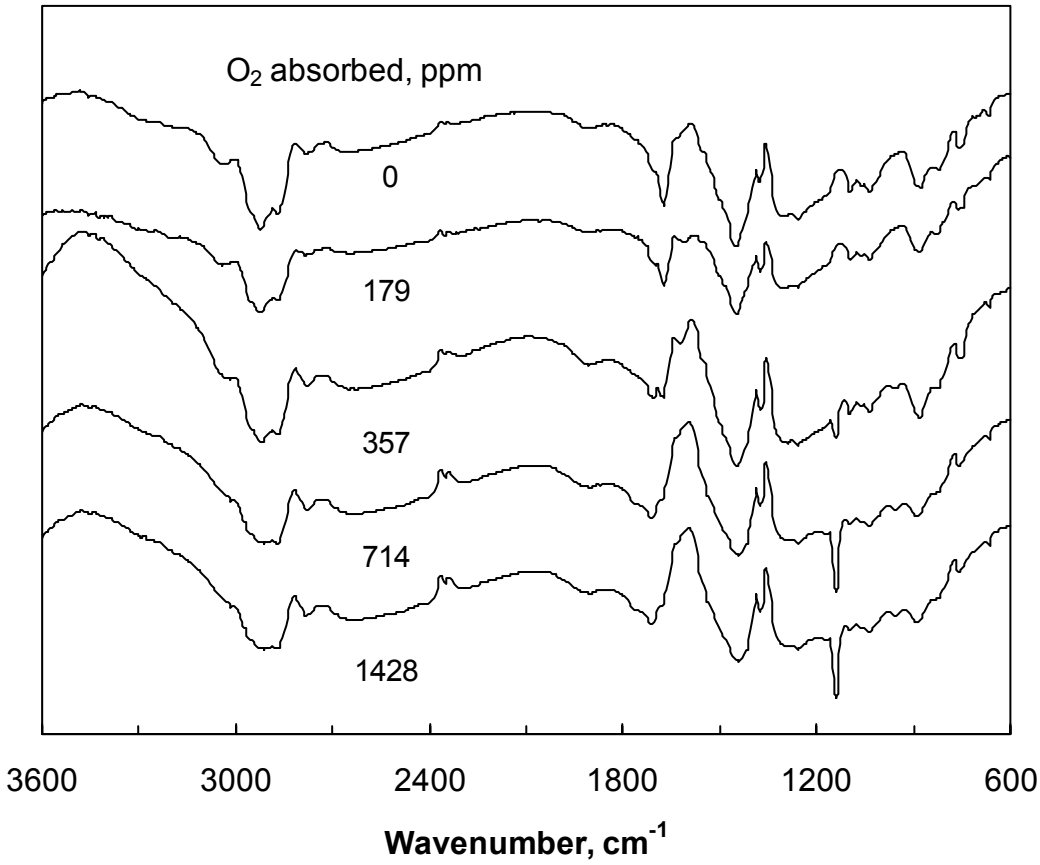

Figure 4.3: DRIFT spectrum of oxidised Refcoals

4.2.1 Diffuse reflectance infrared spectroscopy (DRIFT)

The IR spectra of Refcoal and oxidised Refcoal were recorded on a Perkin-Elmer Spectrum GX FTIR spectrometer (Norwalk, CT, USA) in the range of 4 000 – 400 with 2 cm^{-1} resolutions.

Figure 4.3 shows the DRIFT spectra of the original and oxidised Refcoal samples. These samples were labelled according to the oxygen absorbed by the Refcoal as ppm.

The IR band assignments were taken from the work of (Nosyrev *et al*, 1996) and (Alciaturi *et al.* 1996). With increasing oxidation, changes are observed in the following bands: the OH absorption band region (2 200 – 3 700 cm^{-1}) decreases in intensity; the C=O absorption band region (1 700, 1 740 cm^{-1}) broadens and the absorption maximum shifts to higher wavenumbers; the sharp C-O stretching band (around 1 140) shows a significant increase in intensity. Other bands, e.g. aliphatic

C-H absorption bands (2 920 – 2 840 cm^{-1}) and aromatic C-H stretching bands around (3 037 cm^{-1}), aromatic C-C stretching bands (around 1 471 cm^{-1}), methylene C-H bands in plane bending (around 1 441 cm^{-1}), and aromatic C-H deformation bands (between 740 and 874 cm^{-1}) are observed but were not affected (Sharma and Gihar, 1991).

4.2.2 Nuclear magnetic resonance

Figures 4.4(a) and (b) show the ^{1}H NMR spectra for abietic acid and diabietic acid.

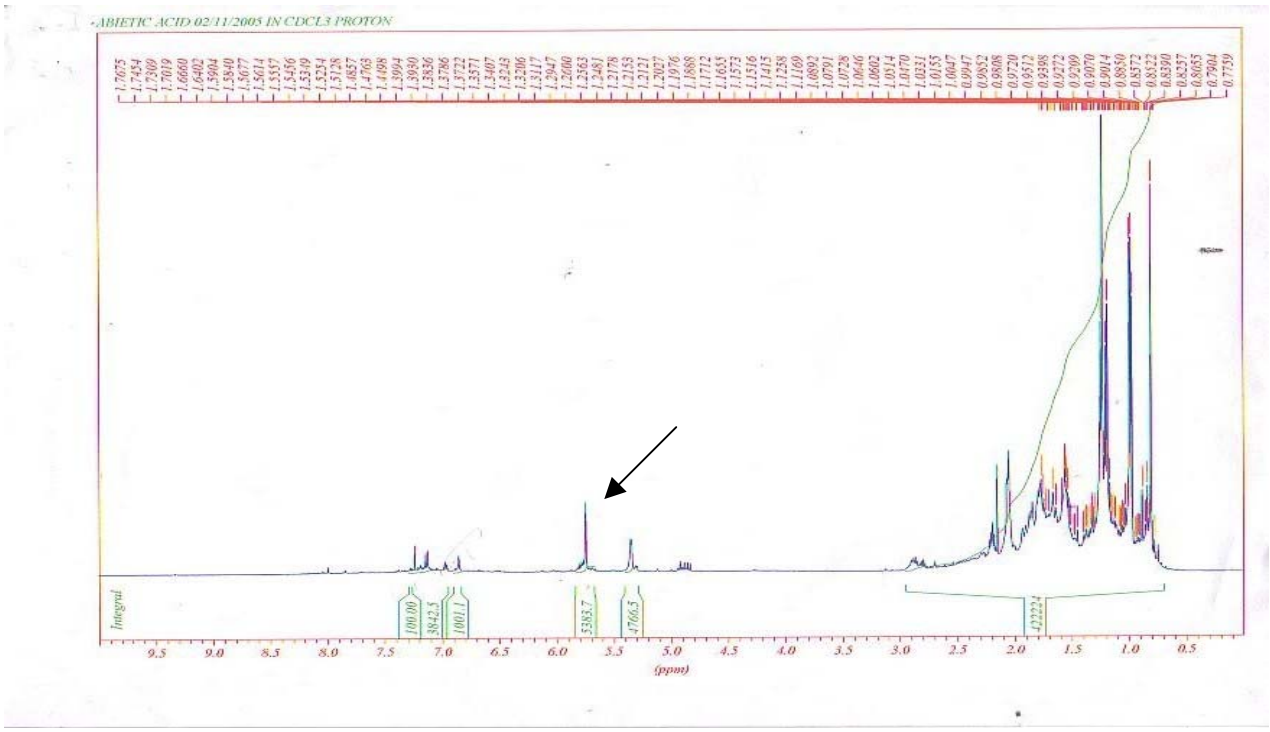

Figure 4.4(a): ^{1}H NMR spectra of abietic acid

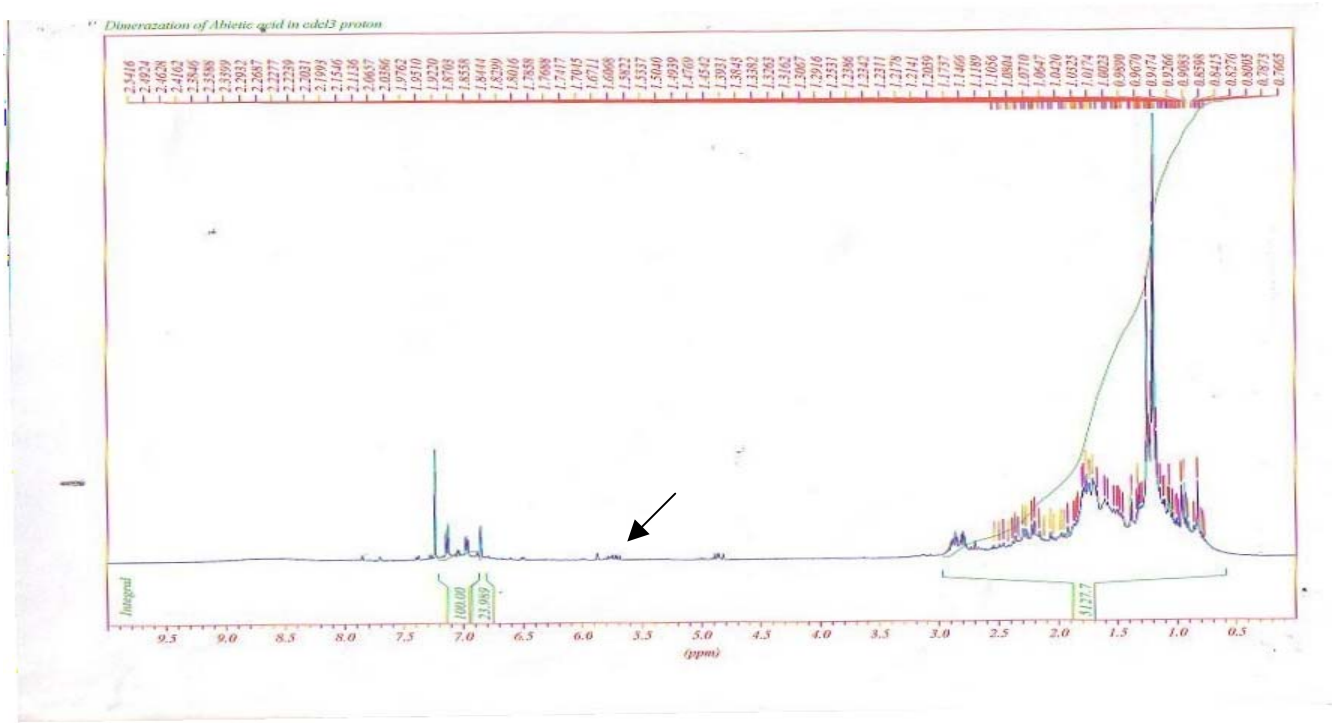

Figure 4.4(b): ^{1}H NMR spectra of the abietic acid dimer

Theoretically, the peak at 4.38 ppm should be half of its original size after dimerisation because the hydrogen in the olefinic position should be half the original amount, as can be seen in the structure (Figure 4.4(a) and (b)). To determine this, the area under the NMR curve is used as this indicates the amount of a particular species in a sample. The peak of the original sample had an area of 4.74% (of the total area), which showed the amount of hydrogen in the olefinic position, and the dimer had an area of 2.24%. This suggests that dimerisation of the abietic acid did take place.

4.3 THERMAL GRAVIMETRIC ANALYSIS (TG)

The thermal stability of abietic acid, diabietic acid (neat and carbonised) and Refcoal or Refcoal plus diabietic acid (neat, oxidised and carbonised) as determined by thermal gravimetric analysis (TGA) is reported in Figures 4.5(a) to (c).

Figure 4.5(a) shows the TGA curves for abietic and diabietic acid. The DTG curve for the latter reveals that mass loss occurs in three distinct steps. The onset of the first step is at 128 ºC. The loss between 89 and 167 °C amounts to ca. 8% and probably reflects the loss of moisture from the sample. For both acids, most of the mass loss occurs during the two overlapping mass-loss events located near 300 °C and 430 °C. These mass-loss events start at 178 ºC and are complete at ca. 520 ºC. The first probably reflects the vaporisation of the acids, while the other one also involves pyrolysis. At this point the remaining char, in the case of diabietic acid, constitutes only 3,7% of the initial sample mass. Virtually no mass remains on reaching ca. 700 ºC. These results show that both acids are very poor char-formers, but clearly show that mass loss occurs more slowly for the dimer.

It was therefore decided to carbonise the dimer acid in a sealed glass tube. The pyrolysis was conducted at 600 °C for 3 hours. The yield of char was ca. 98%. The TG result for this product, in an N_2 atmosphere, is shown in Figure 4.5(b). It shows a very low volatility below 500 °C. Mass loss to 1 000 °C amounted to less than 5,5%.

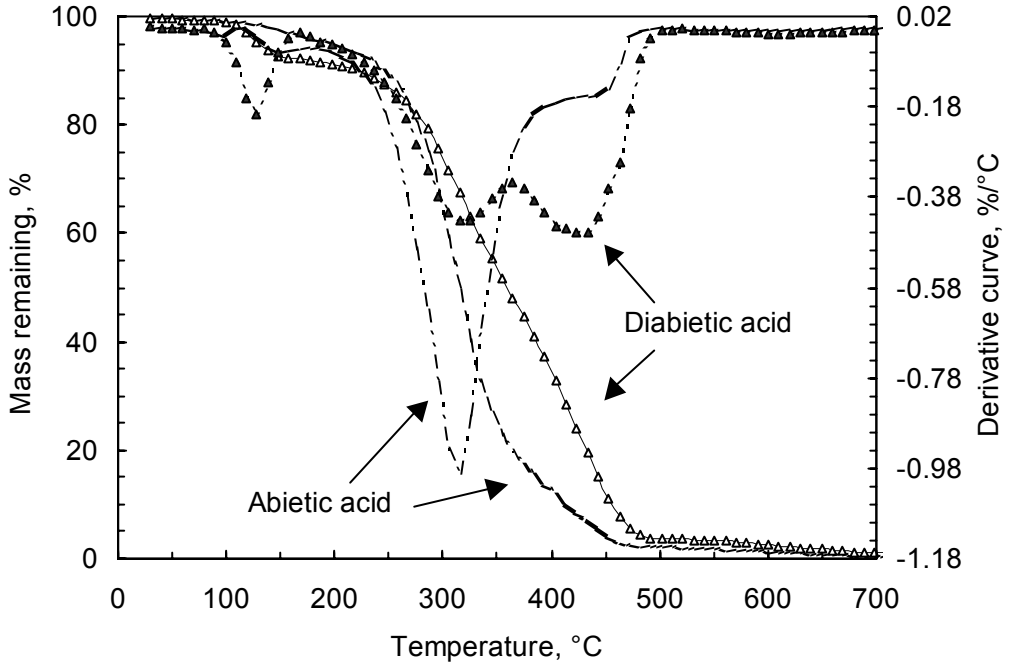

Figure 4.5(a): TG and DTG curves of neat abietic and diabietic acid obtained in N_2

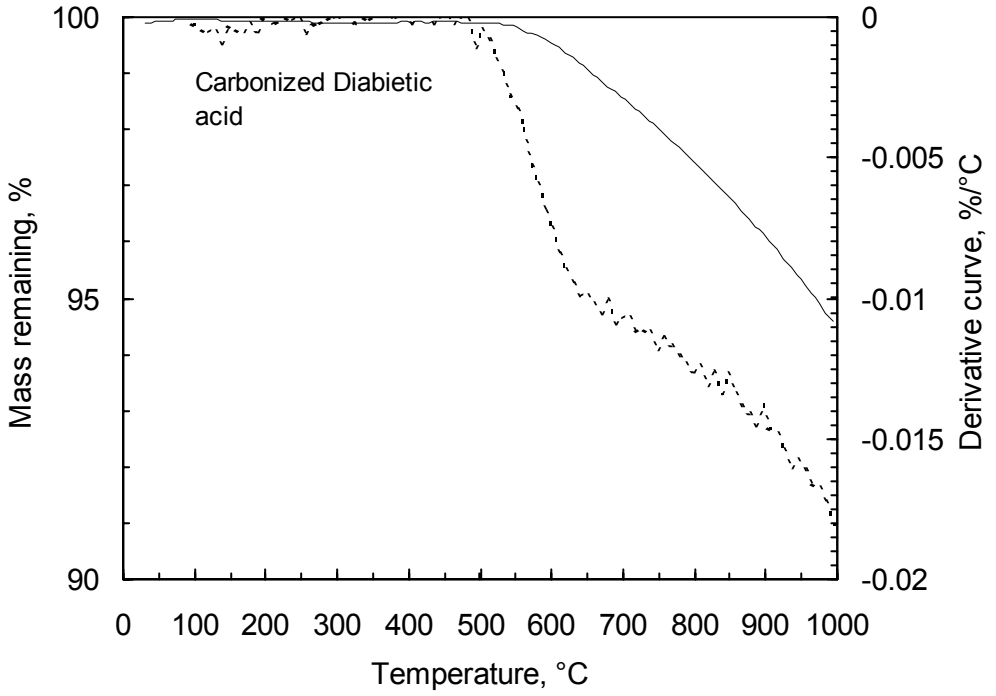

Figure 4.5(b): TG and DTG curves obtained in N_2 for of diabietic acid carbonised in a sealed quartz tube at 680 °C for 5 h

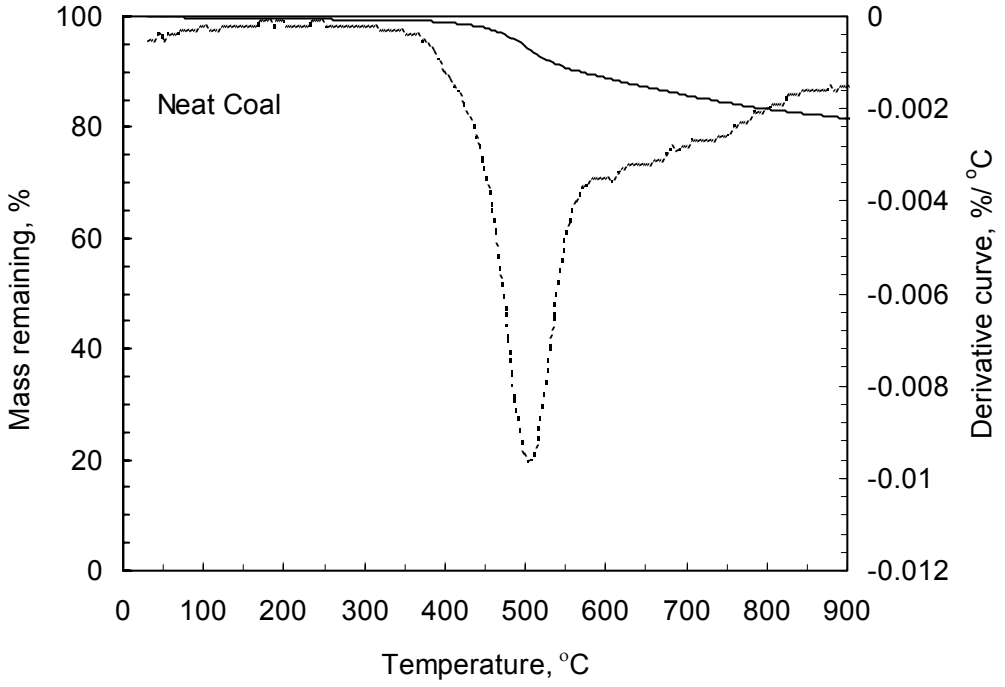

Figure 4.5(c): TG and DTG curves of neat coal (precursor) obtained in N_2

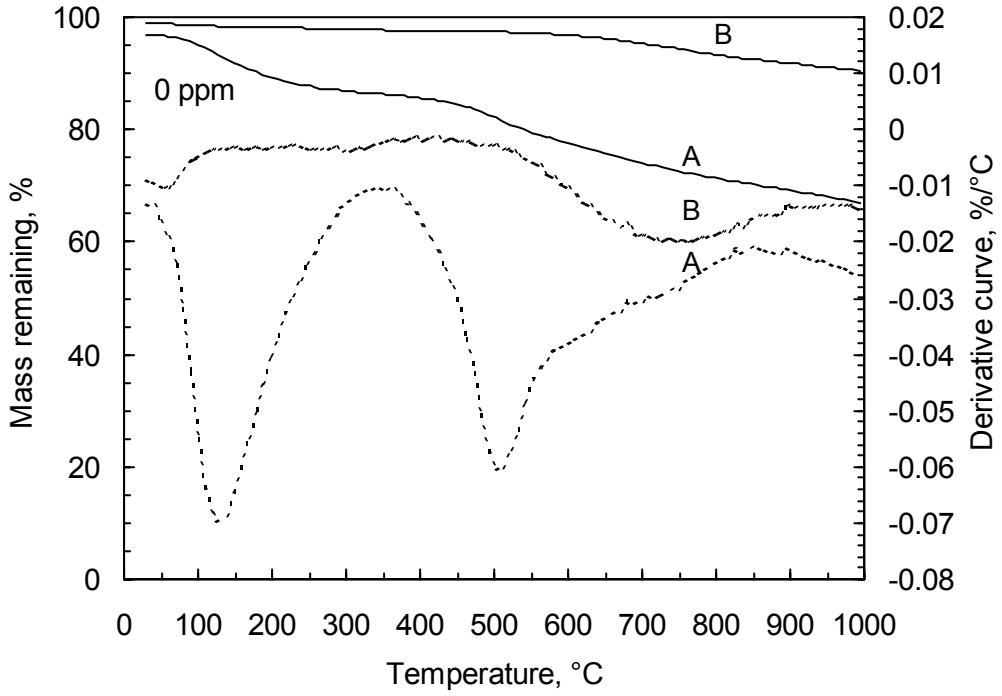

Figure 4.6(a): Comparison of the TG and DTG curves obtained in N_2 for (A) Refcoal and (B) Refcoal carbonised at 680 °C for 5 h

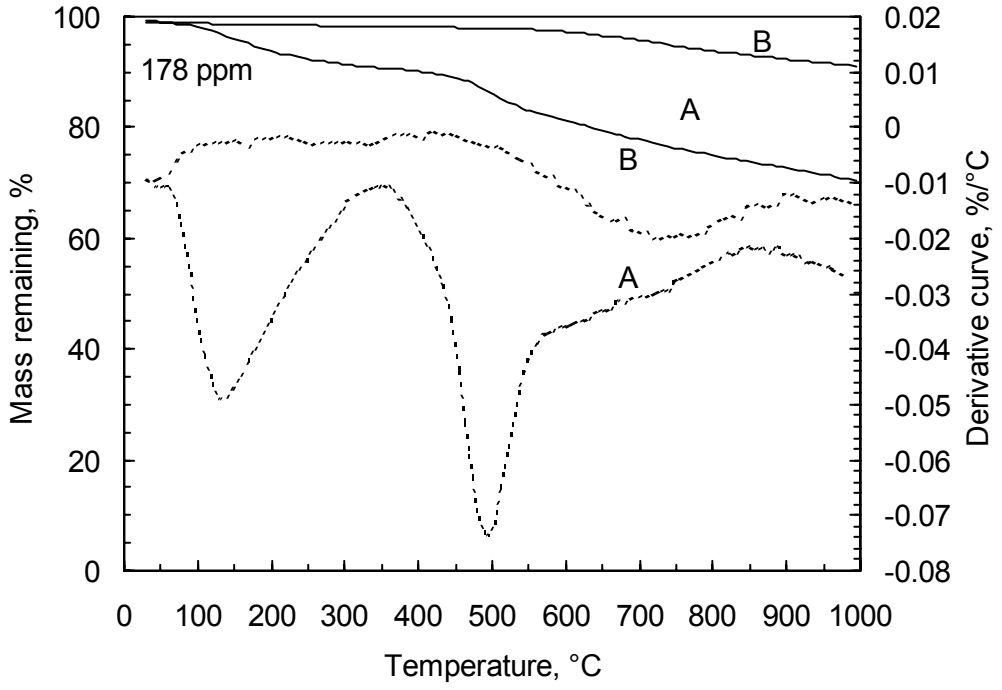

Figure 4.6(b): TG and DTG curves obtained in N_2 for (A) oxidised Refcoal and (B) oxidised Refcoal carbonised at 680 °C for 5 h

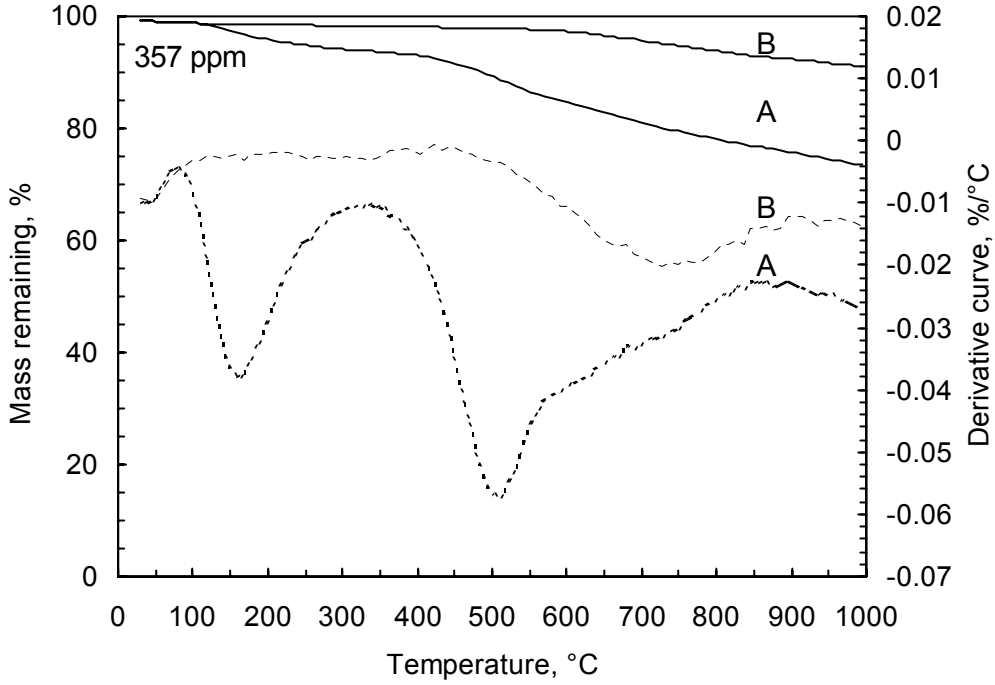

Figure 4.6(c): TG and DTG curves obtained in N_2 for (A) oxidised Refcoal (B) oxidised Refcoal carbonised at 680 °C for 5 h

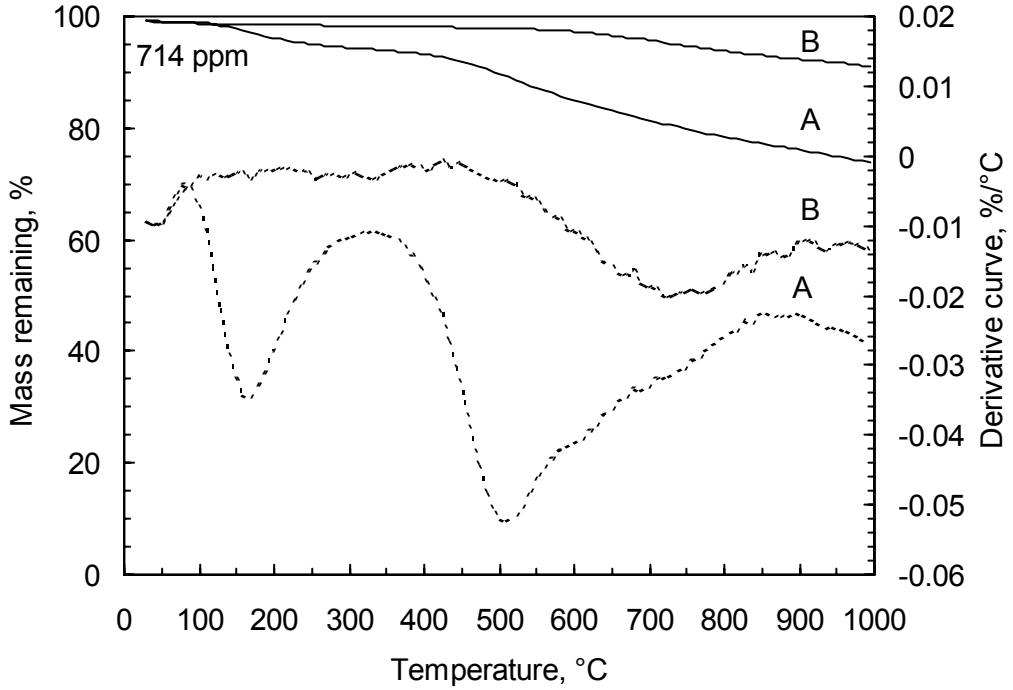

Figure 4.6(d): TG and DTG curves obtained in N_2 for (A) oxidised Refcoal and (B) oxidised Refcoal carbonised at 680 °C for 5 h

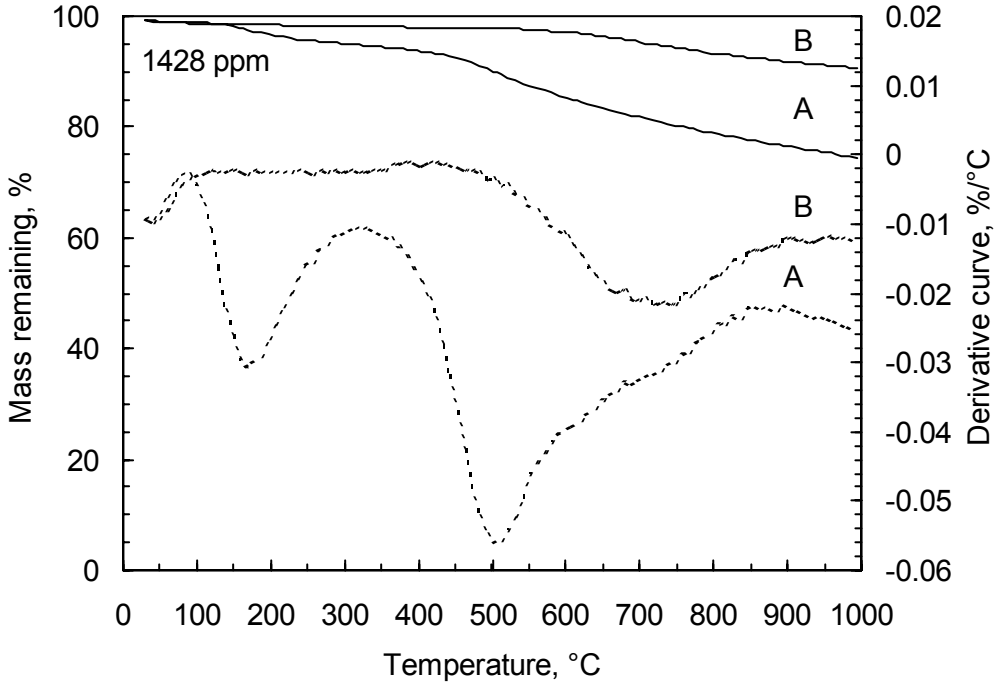

Figure 4.6(e): TG and DTG curves obtained in N_2 for (A) oxidised Refcoal and (B) oxidised Refcoal carbonised at 680 °C for 5 h

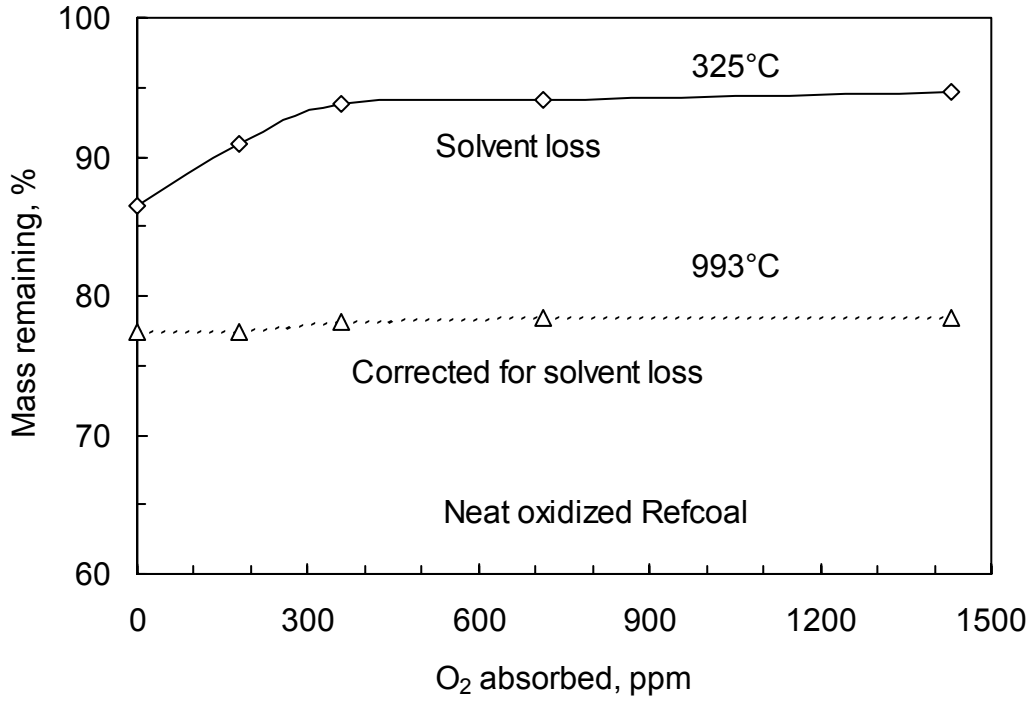

Figure 4.7(a): Summary of TG and DTG curves obtained in N_2 for oxidised Refcoal

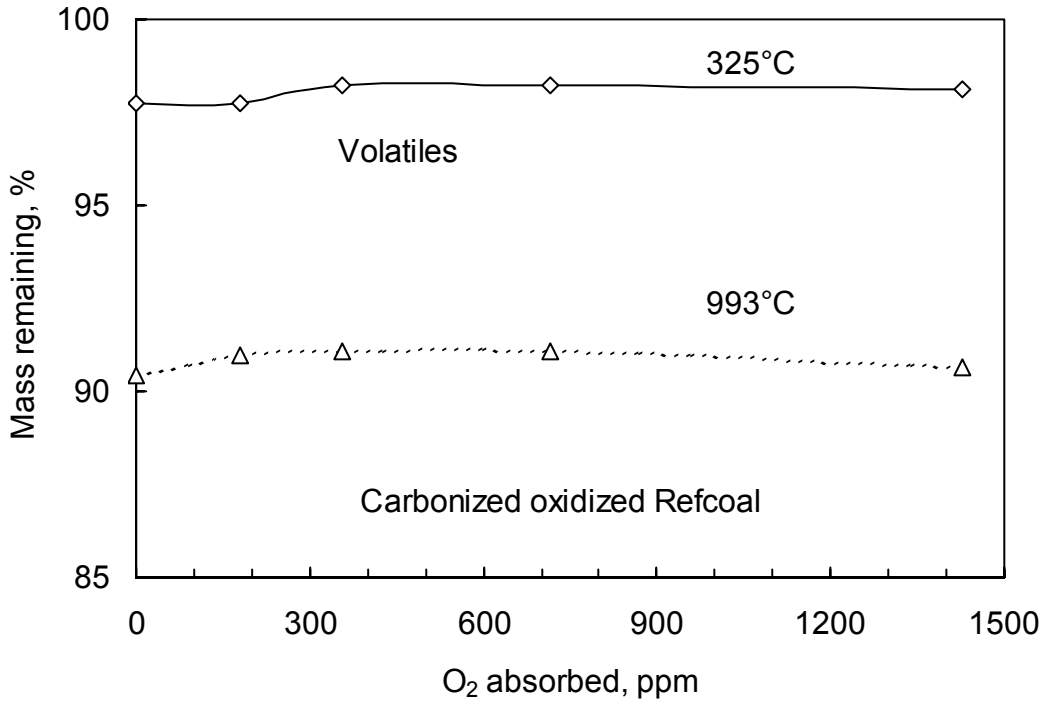

Figure 4.7(b): Summary of TG and DTG curves obtained in N_2 for carbonised oxidised Refcoals at 680 °C for 5 h

Figures 4.6(a) to (e) show that mass loss of Refcoal and oxidised Refcoals take place in three steps. The first step is essentially complete by 325 ^{O}C and represents the vaporisation of the solvent DMF. The next two mass-loss events overlap, but their peak rates occur at ca. 500 ^{O}C and 750 ^{O}C. Figures 4.7(a) and (b) summarise the effect of Refcoal oxidation on the observed mass loss as a function of temperature. The results show that Refcoal is a very good char-former, yielding residues exceeding 66% and 90% for the neat and carbonised forms respectively. Low to moderate oxidation improves the char yields for the uncarbonised Refcoals. Note that all ppm values are refferring to degree of oxidation. Above the 300 ppm O_2 level of oxidation there is no further improvement. Oxidation had little effect on the char yield of the carbonised samples (Figure 4.7(b)).

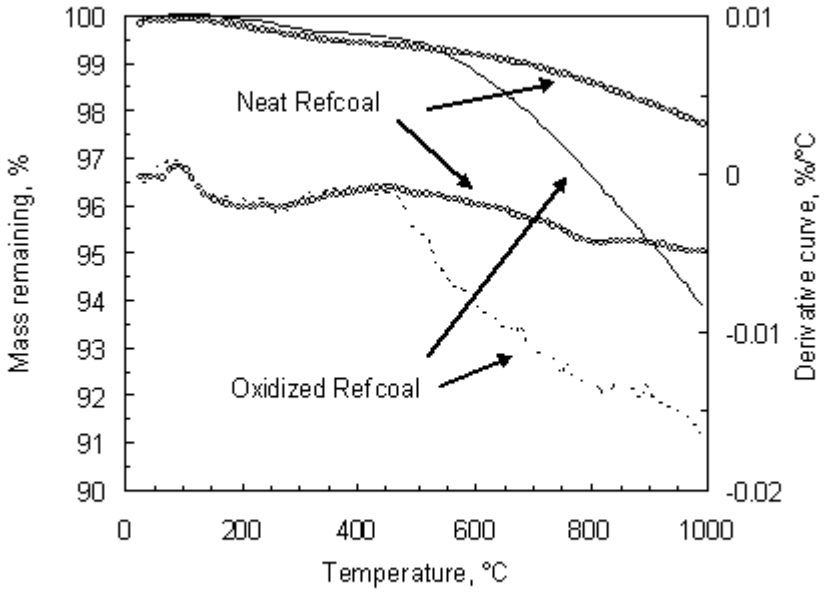

Figure 4.8: TG and DTG curves obtained in N_2 for Refcoal and oxidised Refcoal carbonised at 680 °C for 5 h

Both samples contained 10% diabietic acid

Figure 4.8 shows the TGA curve for Refcoal and oxidised Refcoal, both with diabietic acid as additive. The thermal behaviour of these two samples coincides up to a temperature of ca. 500 ˚C. Thereafter the oxidised Refcoal shows, as expected, a greater mass loss. Nevertheless, both these samples gave enhanced char yields (ca. 98 and 94% respectively), which were obtained in the absence of diabietic acid (ca. 90%). It is concluded that the diabietic acid aids char formation in both the neat and oxidised Refcoal.

4.4 RAMAN SPECTROMETRY

Figures 4.9(a) to (d) show the Raman spectra of the carbonised samples. All ppm values are referring to degree of oxidation.

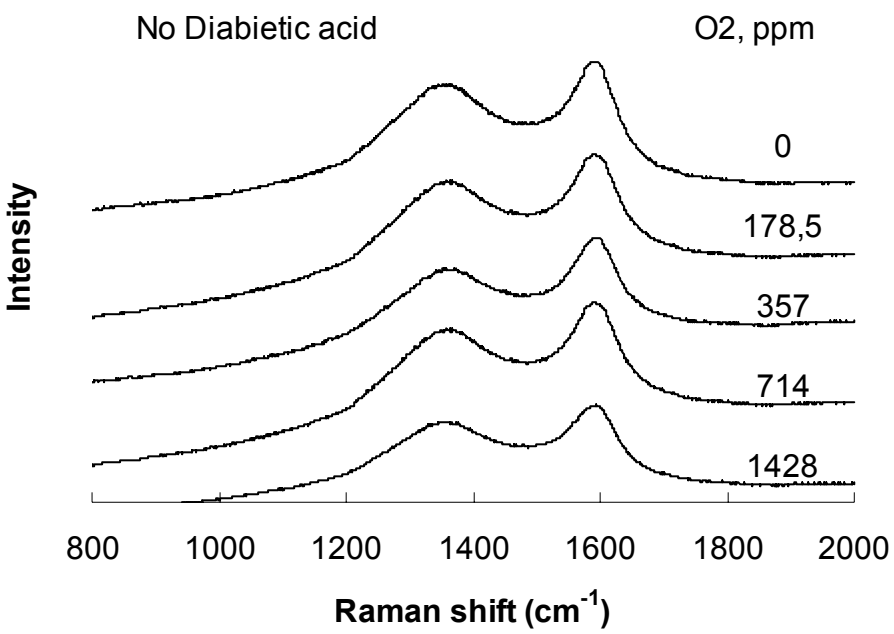

Figure 4.9(a): Raman spectra of oxidised Refcoal cokes

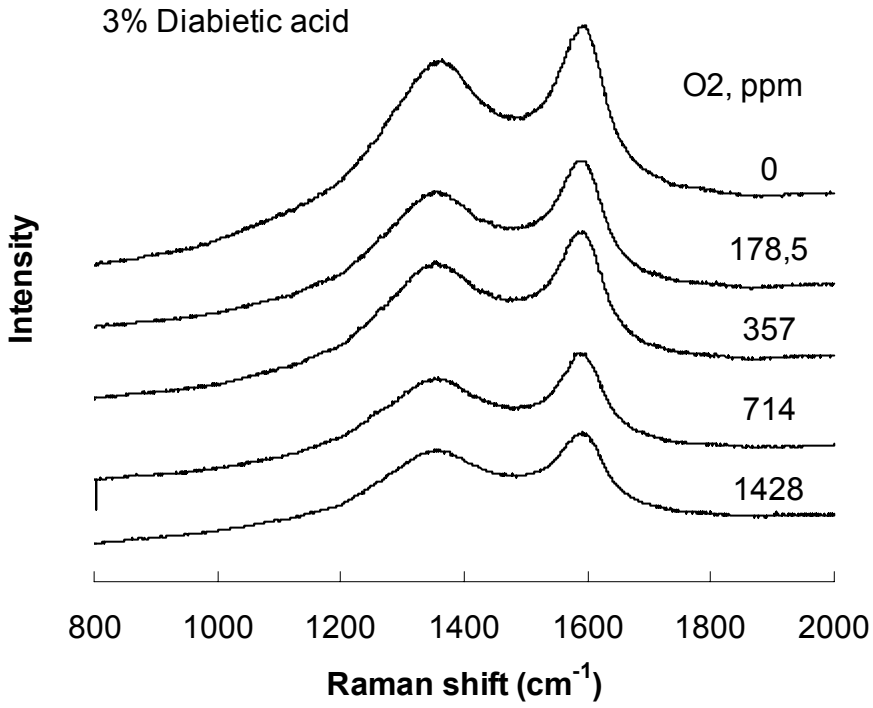

Figure 4.9(b): Raman spectra of oxidised Refcoal cokes treated with 3% diabietic acid

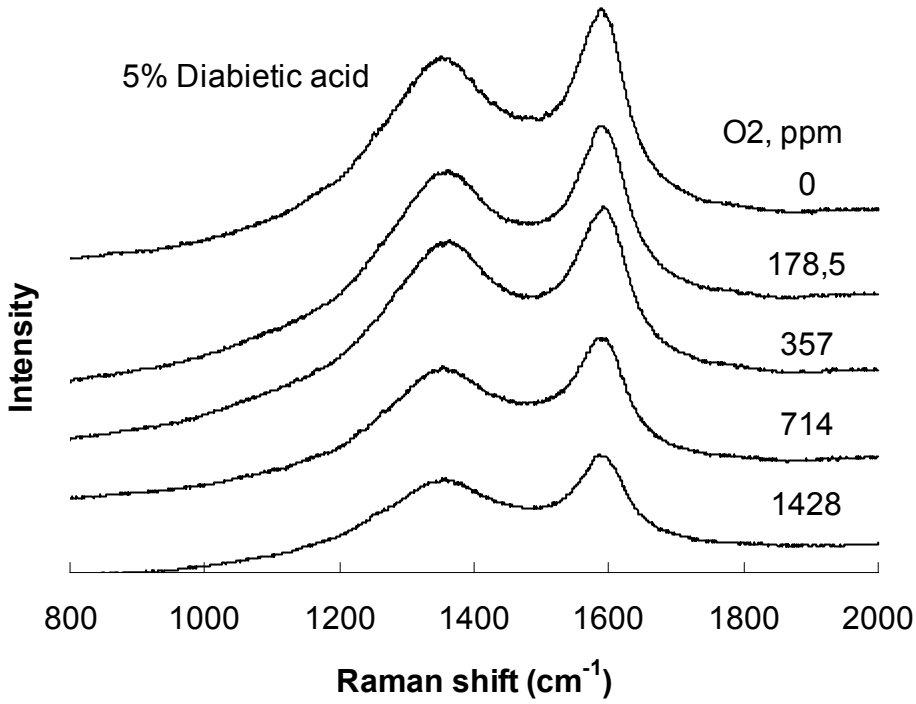

Figure 4.9(c): Raman spectra of oxidised Refcoal cokes treated with 5% diabietic acid

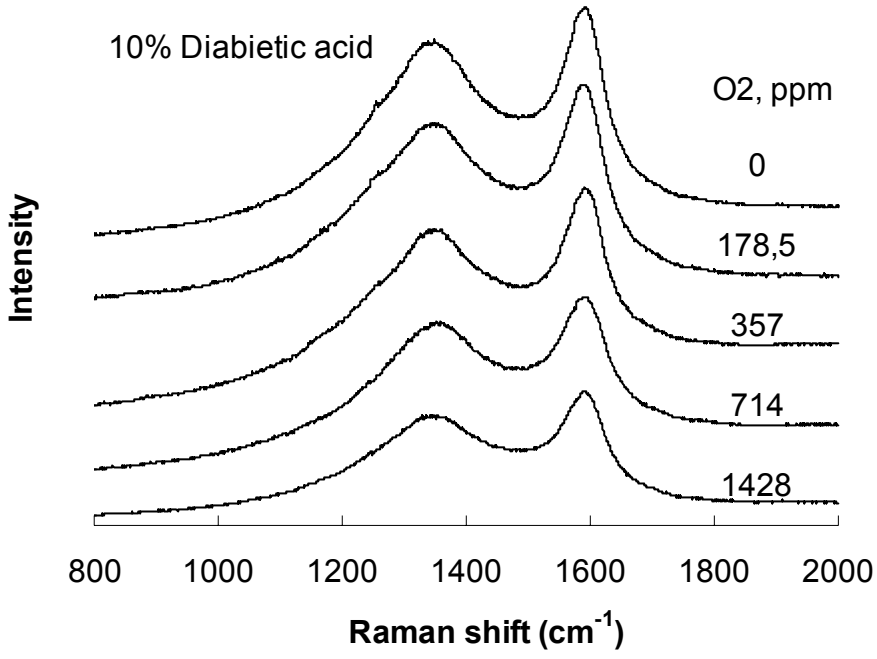

Figure 4.9(d): Raman spectra of oxidised Refcoal cokes treated with 10% diabietic acid

The Raman spectra of all the carbonised samples are shown in Figures 4.9(a) to (d). They show the characteristic D- and G-bands centred at 1 480 and 1 580 cm^{-1} respectively. They reflect contributions from "disordered carbon" and "graphitic carbon" phases in the material. This means that pure graphite shows only the G-band. The relative intensity of these bands ($R = I_D / I_G$) is also affected by crystal size; they were used here to get a semi-quantitative estimate of the graphite crystallinity of the carbonised oxidised Refcoal samples (Falcon, 1978). The smallest R-value suggests a graphitic structure, while the high R-value suggests a turbostratic structure. The results are shown in Figure 4.10. They reveal that the oxidation had little effect, although the sample containing 357 ppm O_2 is slightly more graphitic. The results obtained for samples doped with diabietic acid show scatter around these values and no definite conclusion could be drawn regarding the influence of the hydrogen donor on graphitisation.

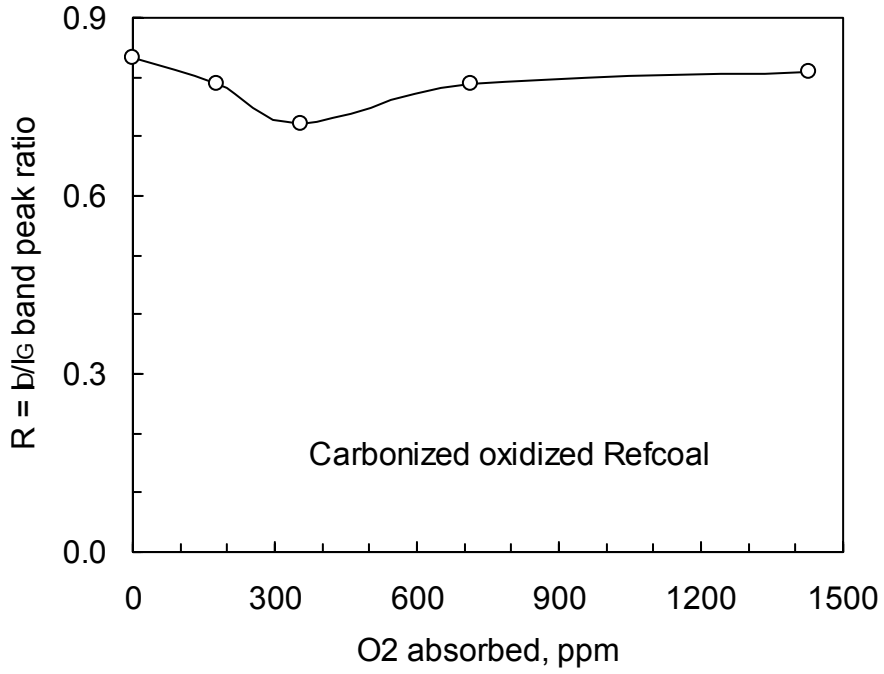

Figure 4.10: Intensity ratios of the G- to D-peaks observed in the Raman spectra of oxidised Refcoal cokes

4.5 X-RAY DIFFRACTION (XRD)

Figure 4.11 shows the X-ray diffraction patterns of the carbonised samples. There are two broad diffraction peaks around $2\theta = 29^{\circ}$ and $2\theta = 52^{\circ}$ in each spectrum. These two peaks correspond to diffraction from the (002) and (004) planes respectively.

It is generally expected that adding diabietic acid on Refcoal and oxidised Refcoal promote the growth of graphitic microcrystallites and sharperns the XRD peak. The (002) peak of oxidised Refcoal is slightly sharper than the others, but the (002) peak broadens and the (004) peak grows to some extent, suggesting that the crystallinity is increasing in the carbonised sample treated with diabietic acid. The surprising observation is that the neat diabietic acid yielded a more graphitic char than Refcoal.

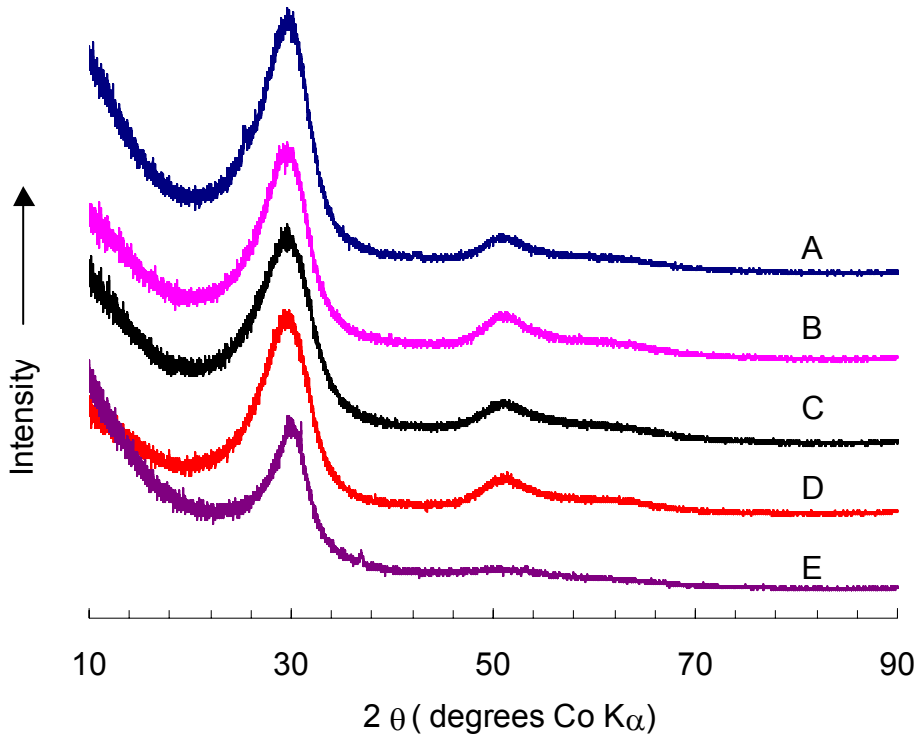

Figure 4.11: The XRD spectra of carbonised (A) diabietic acid (B) Refcoal with 10% diabietic acid (C) Refcoal (D) oxidised Refcoal with 10% diabietic acid and (E) oxidised Refcoal

4.6 OPTICAL MICROSCOPY

The micrograph of diabietic acid in Figure 4.12 shows coarse ribbon anisotropic texture and is also transitional into a mesophase mixed-layer-type structure. These types of coke are normally derived from a petroleum feedstock that is transitional into a mesophase mixed-layer-type structure.

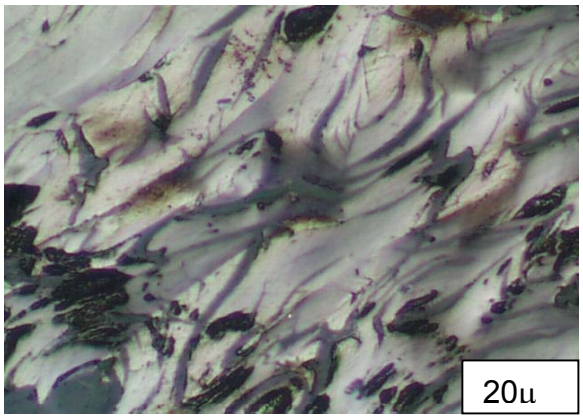

Figure 4.12: Optical micrograph of carbonised diabietic acid

The micrograph of oxidised Refcoal cokes in Figure 4.13(a) shows fine-grained anisotropic texture. This type of carbon is typical of medium bituminous coal. As the Refcoal becomes oxidised, the anisotropy texture is reduced and the pores develop. Note that ppm labels refer to degree of oxidation. The fully oxidised Refcoal (1 428 ppm) is isotropic and has some cracks, whereas the slightly oxidised Refcoal (178.5 ppm) shows a medium granular anisotropic texture with no pores.

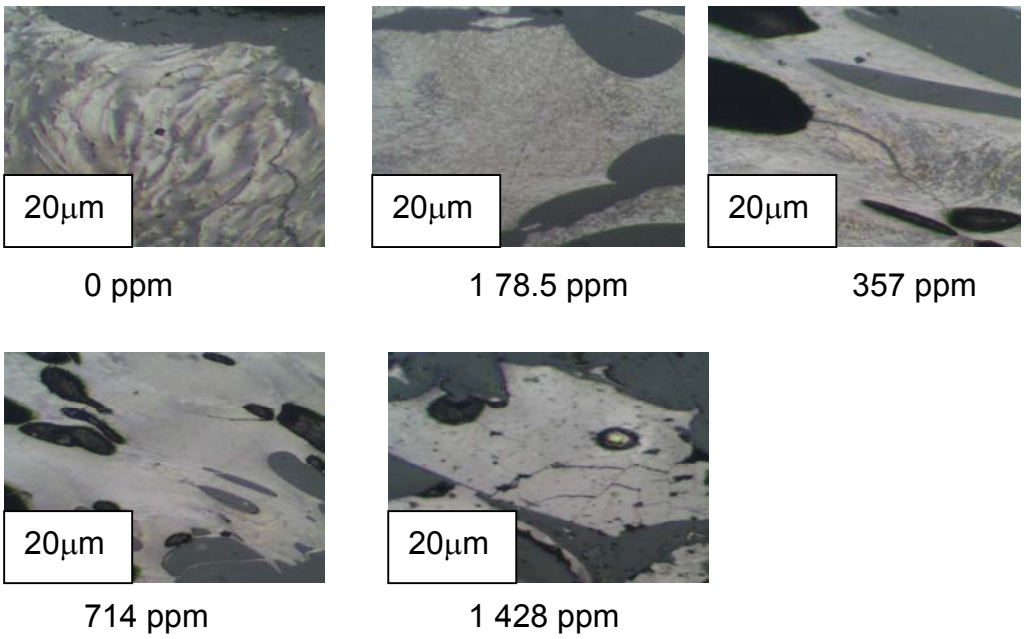

Figure 4.13(a): Optical micrograph of oxidised Refcoal cokes

Figure 4.13(b) shows the medium granular anisotropic structure, without any pores, while Figures 4.13(c) and (d) show the coarse lenticular anisotropic structure formed by the mesophase.

This shows that as the amount of diabietic acid increases in oxidised Refcoal, the anisotropic texture improves. The improvement of the anisotropic texture can be clearly seen on a fully oxidised Refcoal.

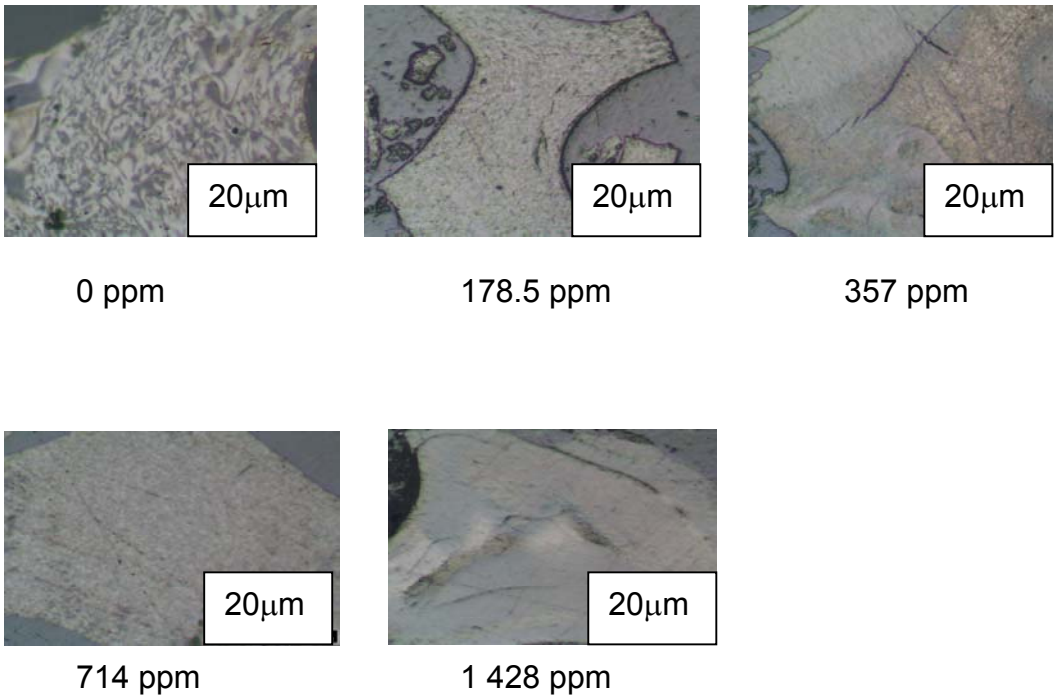

Figure 4.13(b): Optical micrograph of oxidised Refcoal cokes treated with 3% diabietic acid

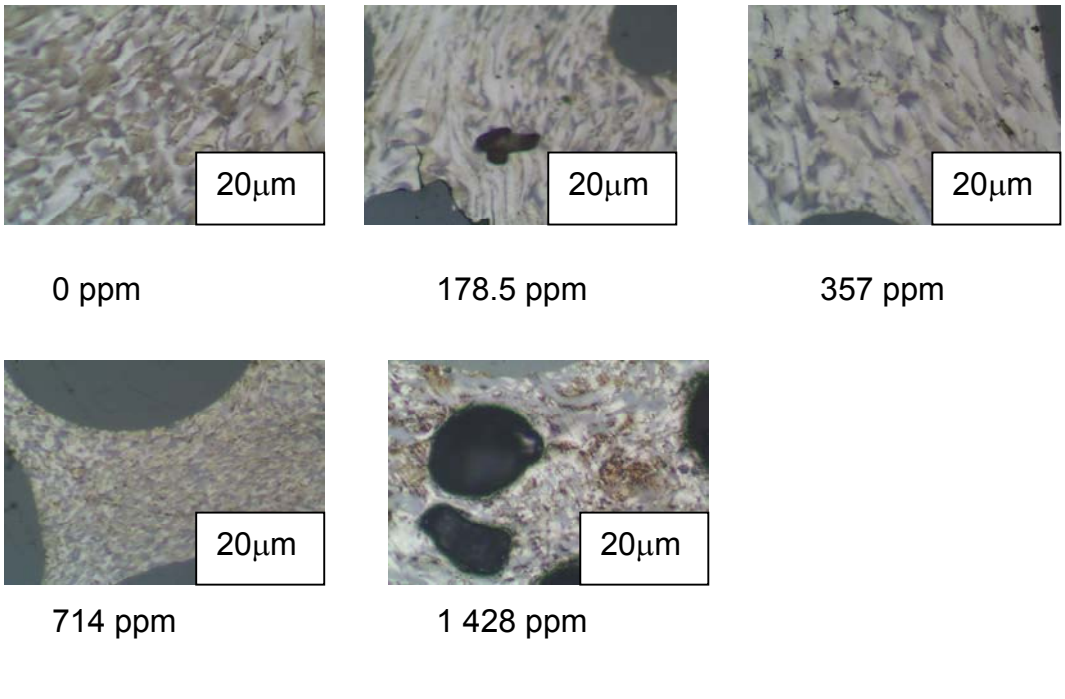

Figure 4.13(c): Optical micrograph of oxidised Refcoal cokes treated with 5 % diabietic acid

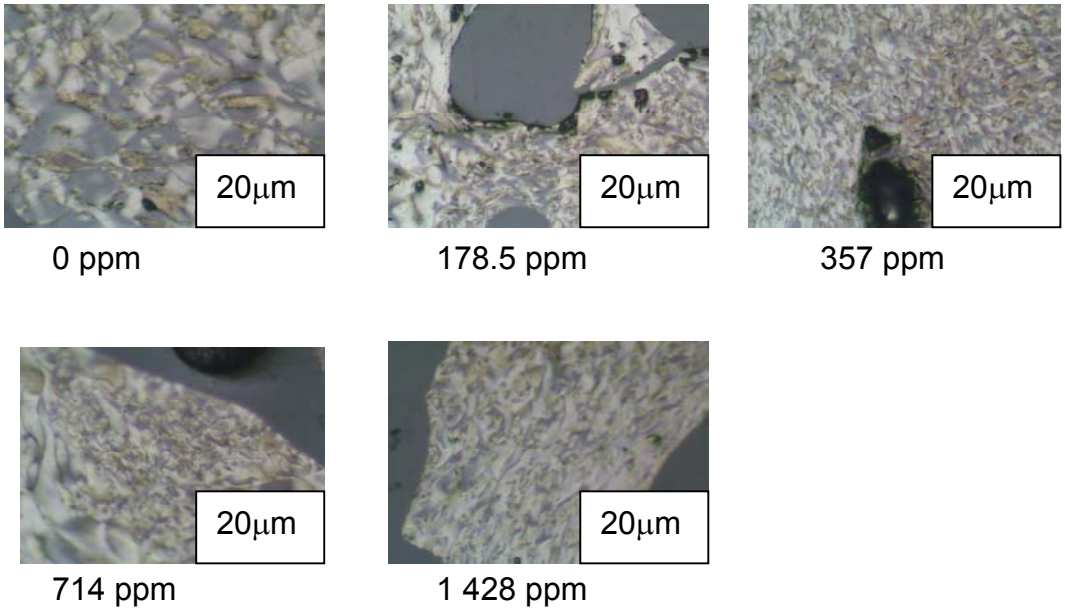

Figure 4.13(d): Optical micrograph of oxidised Refcoal cokes treated with 10% diabietic acid

CHAPTER 5: CONCLUSIONS

Refcoal is a refined carbon precursor obtained by extracting coal using a combination of DMF and sodium hydroxide. Neat Refcoal yields anisotropic cokes by pyrolysis. However, the Refcoal solution easily takes up oxygen. Such oxidised Refcoal yields isotropic cokes. Unlike anisotropic cokes, these isotropic cokes do not graphitise easily. The main purpose of this study was to produce anisotropic cokes from oxidised Refcoal using diabietic acid as a hydrogen donor additive.

Tshikondeni coal samples were extracted to produce solutions that contained about 8% 'carbon' solids. The solute was oxidised by allowing it to react with predetermined amounts of oxygen. The highest degree of oxidation achieved was 1 428 ppm O_2 based on the Refcoal solids. Oxidation was confirmed by DRIFT analysis. The intensity of the hydroxyl bands (3 200 – 3 700 cm^{-1}), aromatic stretching bands (1 600 cm^{-1}), carbonyl bands (1 700 – 1 740 cm^{-1}) and ether bands (1 120 – 1 160 cm^{-1}) changed with the increasing oxygen content.

The pyrolysis carbon yield was determined using TGA under a nitrogen atmosphere at 1 000 ˚C. Neat Refcoal gave a carbon yield of 77% (corrected for solvent loss). Oxidation had little effect on this value. Similarly, neat carbonised (680 ˚C) Refcoal gave a carbon yield of 92.5% at ca. 1 000 ˚C and again oxidation did not affect this yield. Carbonised samples containing 10% diabietic acid improved the carbon yield to 98% for the neat Refcoal and to 94% for the fully oxidised Refcoal. Diez *et al*. (1999) suggested that hydrogen donors, e.g. diabietic acid, stabilise radicals and thereby promote the growth of aromatic molecules.

The carbonised samples were also investigated using Raman spectroscopy and XRD. The graphite peak (G-peak) in the Raman spectra decreased with increasing Refcoal oxygen content. XRD indicates that addition of diabietic acid improves the crystallinity of the coke. This was expected but surprisingly it was also found that carbonising neat diabietic acid yields a more crystalline coke than is obtained from samples containing Refcoal.

Optical microscopy revealed that the cokes become less anisotropic as the Refcoal is oxidised. Adding diabietic acid influences the optical texture of the cokes in that they become more anisotropic.

It is concluded that addition of diabietic acid to oxidised Refcoals makes the resulting cokes more anisotropic. It is postulated that the mechanism involves the acid acting as a hydrogen donor, stabilising aromatic radicals and facilitating their polymerisation.

CHAPTER 6: REFERENCES

Alciaturi, C.A., Escobar, M.E. and Vallejo, R. 1996. Prediction of coal properties by derivative DRIFT spectroscopy. *Fuel*, **75**: 491-499.

American Society for Testing and Materials (ASTM). 1979. *Annual Book of Standards. Part* 26*. Gaseous Fuels, Coal and Coke*.

Aranda, F.J. and Villalaín, J. 1997. The interaction of abietic acid with phospholipid membranes. *Biochimica et Biophysica Acta,* **1327**: 171-180.

Berkowitz, N. 1979. *An Introduction to Coal Technology.* New York, London: Academic Press.

Bodily, D.M. Wann, J-P. and Kopp, V. 1986. *Solvent swelling of coal and coal macerals*. Poster session, printed for the meeting of the Division of Petroleum Chemistry, American Chemical Society, Salt Lake City, 7-12 September 7-12.

Brooks, J.D. and Taylor, G.H. 1965. The formation of graphitising carbons from the liquid phase. *Carbon*, **3**: 185-193.

Brooks, J.D and Taylor, G.H. 1968. *Chemistry and Physics of Carbon*. Ed. P.L. Walker, Chapter 4 London: Edward Arnold, p 243.

Bundy F.P., Basset, W.A., Weather, M.S., Hemley, R.J., Mao, H.K. and Goncharov, A.F. 1996. The pressure-temperature phase and transformation diagram for carbon. *Carbon*, **34**: 141-148.

Carpenter, A.M. 1988. *Coal Classification.* London: IEA Coal Research, p 104.

Chaudhuri, S.G., Choudhury, N.B.S., Bhatt, D.M., Ghose, S.P., Chatterjee, D.S. and Mukherjee, D.K. 1997. The influence of pressure and hydrothermal treatment on the microtextural characteristics of coke. *Carbon*, **35**: 1457-1464.

Chunlan, L., Shaoping, X., Yixiong, G., Shuqin, L. and Changhou, L. 2005. Effect of pre-carbonisation of petroleum cokes on chemical activation process with KOH. *Carbon*, **43**: 2295-2301.

Collin, W.R. 1984. *Coal Geology and Coal Technology*. University of New South Wales, Australia, p 123.

Cottinet, D., Couderc, P. and Saint Romain, J.L. 1988. Raman microprobe study of heat-treated pitches. *Carbon*, **26**: 339-334.

Dekker, M. *Coal Handbook, Energy, Power and Environment.* 1981. Chapter 11, New York.

Delhaès, P. 1979. *Graphite and Precursors*. Netherlands: Gordon and Breach.

Díez, M.A., Domínguez, A., Barriocanal, C., Alvarez, R., Blanco, C.G. and Canga, C.S. 1999. Hydrogen donor and acceptor abilities of pitches from coal and petroleum evaluated by gas chromatography. *Journal of Chromatography A*, **830**: 155-164.

Druz, B., Zaritsky, I., Yevtukhov, Y., Konchits, A., Valakh, M., Shanina, B., Kolesnik, S., Yanchuk, I. and Gromovoy, Y. 2004. Diamond-like carbon films: Electron spin resonance (ESR) and Raman spectroscopy. *Diamond and Related Materials*, **13**: 1592-1602.

Dumont, M., Dourges, M.A., Bourrat, X., Pailler, R., Naslain, R., Babot O., Birot, M. and Pillot, J.P. 2005. Carbonisation behaviour of modified synthetic mesophase pitches, *Carbon*, **43**: 2277-2284.

Encyclopedia of Physical Science and Technology. 1987, London: Academic Press. Vol. 3: 3-71.

Encyclopedia of chemical technology. 1994, New York: Wiley . Vol. 5-8.

Eser, S. and Hou, L. 1996. Letters to the Editor, 3-D H NMR imaging of porosity in calcined needle cokes. *Carbon*, **34**: 805-831.

Falcon, R.M.S. 1978. Coal in South Africa. Part 2: The application of petrography to the characterisation of coal. *Mineral Science and Engineering*, p 10.

Gibson, J. and Gregory, D.H. 2000. *Carbonisation of Coal*. Oxford, UK: Mills & Boon Limited.

Giri, C.C. and Sharma, D.K. 2000. Kinetic studies and shrinking core model on solvolytic extraction of coal. *Fuel Processing Technology*, **68**: 97-109.

Gonzalez, D., Montes-Moran, M.A., Yong, R.J. and Garcia, A.B. 2002. Effect of temperature on the graphitisation process of a semianthracite. *Fuel Processing Technology*, **79**: 245-250.

Granfield, J. and Buckman, D. 1978. *Coal.* UK: Wayland Publishers Limited.

Greyvenstein, G.P. and Rousseau, P.G. 2003. Design of physical model of the PBMR with the aid of Flownet. *Nuclear Engineering and Design,* **2798**: 1-11.

Grint, A., Mehani, S., Trewhella, M. and Crook, M.J. 1985. Role and composition of the mobile phase in coal. *Fuel*, **64**: 1355-1361.

Honda, H. 1988. Carbonaceous mesophase: History and prospects. *Carbon*, **26**: 39-156.

Hugh, O.P. 1993. *Handbook of Carbon, Graphite, Diamond and Fullerene: Properties, Processing and Application*. USA: Noyes Publications.

International Committee for Coal Petrology. 1963. *Handbook of Coal Petrography.* 2nd edition, Paris: Centre National de la Recherche Scientifique.

Khan, M.A., Ahmad, I., Ishaq, M., Shakirullah, M., Jan, T.M., Eid-ur-Rehman and Bahader, A. 2003. Spectral characterisation of liquefied products of Pakistani coal. *Fuel Processing Technology*, **85**: 63-74.

Koch, A., Gruber, R., Cagniant, D., Pajak, J., Krzton, A. and Duchène, A. 1995. A physicochemical study of carbonisation phases. Part I. Tars migration and coking pressure. *Fuel Processing Technology*, **45**: 135-153.

Koster, A., Matzner, H.D. and Nicholls, D.R. 2003. PBMR design for the future. *Nuclear Engineering and Design*, **222**: 231-245.

Lewis, I.C. and Singer, L.S. *Chemistry and Physics of Carbon*. Vol. 17. New York: Marcel Dekker, p 42.

Lopez, D., Sanada, Y. and Mondragon, F. 1998. Effect of low-temperature oxidation of coal on hydrogen-transfer capability. *Fuel*, **77**: 1623-1628.

Machnikowska, J., Machnikowska, H., Brzozowska, T. and Zielinski, J. 2002. Mesophase development in coal-tar pitch modified with various polymers, *Journal of Analytical and Applied Pyrolysis*, **65**: 147 – 160.

Mantell, M.L. 1968. *Carbon and Graphite Handbook*. New York and London: John Wiley and Sons.

Marsh, H. 1980. *Introduction to Carbon Science*. UK: Butterwoths.

Marsh, H. 2002. *Sciences of Carbon Materials*. Universidad de Alicate.

Marsh, H., Kimber, G.M., Rantell, T. and Scott, E. 1980. Carbonisation and liquid-crystal development. *Fuel*, **59**: 520-521.

Masashi I. 2000. Network structure of coal and association behaviour of coal-derived materials. *Fuel Processing Technology*, **62**: 89-101.

Maya, S., Simoneit, B.R.T, Stojanova, G., Nosyrev, I.E. and Goranova, M. 1995. Composition of the extract from a carboniferous bituminous coal: 1. Bulk and molecular constitution. *Fuel*, **74**: 768-778.

Martínez-Escandell, M. Carriera ,P., Rodríguez-Valero, M.A, Rodríguez-Reinoso, F. 1999. Self-sintering mesophase powder: Effect on extraction/washing with solvent. *Carbon*, **37**: 1662-1665.

Mochida, I., Karai, Y., Nesumi, Y. and Oyama, T. 1986. Carbonisation in a tube bomb. 1. Carbonisation of petroleum residue into a lump of needle coke. *Ind. Eng. Chem. Prod. Res. Dev.,* **25**: 198-201.

Mochida, I., Kudo, K., Fukuda, N., Takeshita, K. and Takahashi, R. 1975. Carbonisation of pitches. IV. Carbonisation of polycyclic aromatic hydrocarbons under the presence of aluminium chloride catalyst. *Carbon*, **13**: 135-139.

Mohindar, S. Ghosh, S.B. and Zondlo, J.W. 1988. Relationship of coal extraction with free radicals. *Fuel Processing Technology*, **18**: 279-286.

Montes-Morán, M.A., Crespo, J.I., Young, R.J., García, R. and Moinelo, S.R. 2002. Mesophase from a coal tar pitch: A Raman spectroscopy study. *Fuel Processing Technology*, **77**: 207-212.

Morgan, D.L. 2000. Nuclear Graphite from Refcoal. CSIR Report 86DC/HtOO2.

Mthembi, P.M. 2003. Coal Purification, MSc thesis, University of Pretoria, Pretoria.

Nicholls, D.R. 2001. The Pebble Bed Modular Reactor. *Trans. Roy. Soc. S. Afr.*, **56**: 125-130.

Nicholls, D.R. 2000. The Pebble Bed Modular Reactor. *South African Journal of Science*, **98**: 31-35.

O'brien, G., Jenkins, B., Estele, J. and Bearth, H. 2003. Coal characterization by automated coal petrography. *Fuel*, **82**: 1067-1073.

Ordóňez, S.,Sastre, H. and Díez, F.V. 2001. Thermogravimetric determination of coke deposits on alumina-supported noble metal catalysts used as hydrodechlorination catalysts. *Thermochimica Acta*, **379**: 25-34.

Pitt, G.J. and Millward, G.R. 1979. *An Introduction to Coal and Modern Coal Processing*. New York: Academic press Philadelphia.

Ramani, C.C., Puranik, P.K. and Dorle, A.K. 1996. Study of diabietic acid as matrix forming material. *International Journal of Pharmaceutics*, **37**: 11-19.

Renganathan K., Zondlo J.W., Mintz E.A., Kneisl P. and Stiller A.H. 1988. Preparation of an ultra low ash coal extract under mild conditions. *Fuel processing technology*, **18**:273-278.

Riddell, F.G. Spark, R.A., Fraser, I.F. and McPherson, I.A. 1997. Effects of abietic acid derivative rosination on C.I. Pigment Yellow 13 *Dyes and Pigments*, **35**: 191-203.

Rodríguez-Reinoso, F., Santana, P., Palazano, E.R., Diez, M.A. and Marsh, H. 1998. Delayed coking: Industrial and laboratory aspects. *Carbon*, **36**: 105-116.

Schapiro, N. and Gray, R.J. 1960. Petrographic classification applicable to coals of all ranks. *Proc. Ill. Min. Inst*., 83-97.

Scott, A.C. 2002. Coal petrology and the origin of coal macerals: A way ahead? *International Journal of Coal Pertrolgy*, **50**: 119-134.

Sharma, D.K. and Gihar, S. 1991. FT-i.r. Spectra of gaseous products from the combustion of pyrotechnic mixtures containing carbon. *Fuel*, **70**: 663-669.

Sharma, D.K. and Singh, S.K, 1995. Extraction of Assam coal through stepwise alkali treatment under ambient pressure conditions. *Fuel Processing Technology*, **45**: 11-25.

Shevkoplyas, V.N. 2002. Coal carbonisation and addition of hydrochloric acid as a way of improving coke quality. *Fuel*, **81**: 947-950.

Sinclair, R.G., Berry, D.A., Schuller, W.H. and Lawrence, R.V. 1970. Influence of reaction conditions on the dimerization of abietic acid and rosin. *Ind. Eng. Chem. Prod. Res. Develop*, **9**: 60-65.

Skoog, D.A. and Holler, F.J. 1992. *Principles of Instrumental Analysis*. London: Sanders College Publishing.

Snyman, C.P. 1976. The petrological composition and origin of coal with special reference to South Africa. *Trans. Geol. Soc. South Africa*, **79**: 242-252.

Starch, E., Mackowsky, H-Th., Teichmuller, M., Tailor, G.H., Chandra, D. and Teichmuller, R. 1982. *Starch's Textbook of Coal Petrology*: Berlin: Gebruder Borntraeger, Stuttgart: Edward Arnold, p 535.

Stopes, M.C. 1935. On the petrology of banded bituminous coals. *Fuel*, **14**: 4-13.

Świetlik, U., Gryglewicz, G., Machnikowska, H., Machnikowski, J., Barriocanal, C., Alvarez, R. and Díez, M.A. 1999. Modification of coking behaviour of coal blends by plasticizing additives. *Journal of Analytical and Applied Pyrolysis*, **52**: 15-31.

Teng, H., Ho, J.A. and Hsu, Y.H. 1997. Preparation of activated carbons from bituminous coals with CO_2 activation-influence of coal oxidation. *Carbon*, **35**: 275-283.

Urban, O., Jehlička, J., Pokornỳ J. and Rouzaud, J.N. 2003. Influence of laminar flow on preorientation of coal tar pitch structural units: Raman microspectroscopic study. *Spectrochimica Acta Part A*, **59**: 2331-2340.

Valkovic, V. 1983. *Trace Elements in Coal*. Boca Raton, Florida: CRC Press, Inc.

Veres, M., Füle, M., Tóth, S., Koós, M. and Pócsik, I. 2004. Surface-enhanced Raman scattering (SERS) investigation of amorphous carbon. *Diamond and Related Materials*, **13**: 1412-1415.

Villalaín, J. 1997. Location of the toxic molecule abietic acid in model membranes by MAS-NMR. *Biochimica et Biophysica Acta,* **1328**: 281-289.

Wilson, P.J. and Wells, J.H. 1950. *Coal, Coke and Coal Chemicals*. New York: McGraw-Hill.

Yokondo, Y., Marsh, H. and Schults, H.D. 1983. *Coal Liquefaction Products, NMR Spectroscopic Characterization and Production Processes*. New York: Wiley, p 125.

APPENDICES

Table A.1: Properties of nuclear-grade graphite

Property	Anisotropic graphite	Isotropic graphite
Density	1.71 g/cm^3	1.86g/cm^3
Resistance	735 μΩ.cm	1 000 μΩ.cm
Tensile strength	9 930 kPa	46 172 kPa
Coefficient of thermal expansion (CTE),10^{-6}/C with grain	2.2	5.3
Coefficient of thermal expansion (CTE),10^{-6}/C against grain	3.8	5.3
Anisotropy ratio (CTE ratio)	1.73	1
Total ash	740 ppm	400 ppm
Boron content	0.4 ppm	0.3 ppm

Table A.2: Physical properties of graphite

Crystalline form	Hexagonal
Lattice parameters	a = 0.246 nm , c = 0.671 nm
Colour	Black
Density at 300 K, 1 atm	2.26 g/cm^3
Atomic volume	5.315 cm^3/mol
Sublimation point at 1 atm (estimated)	4 000 K
Triple point (estimated)	4 200 K
Boiling point (estimated)	4 560 K
Heat of fusion	46.84 kJ/mol
Heat of vaporisation to monoatomic gas	716.9 kJ/mol
Pauling electronegativity	2.5

Table A.3: Uses of coal extracts

Products	Potential customers
Fuel	
Low-ash slurry or solid fuel	Power generation, transportation, domestic heating
High-grade coke	
Electrodes	Steel industry
Anodes	Aluminium industry
Graphite	Nuclear reactors
C-C composites	Military and nuclear

Table A.4: Ultimate analysis of Tshikondeni coal

Element	Coal 1 Wt %	Coal 2 Wt %
Carbon	84.1	81.5
Hydrogen	4.50	4.38
Nitrogen	1.95	1.86
Oxygen	0.46	1.15

Table A.5: Proximate analysis

Moisture (air dry)	0.6
Ash (dry basis)	9.0
Volatile matter (dry basis)	23.3
Fixed carbon (calculation) (dry basis)	67.4
Total sulphur (dry basis)	
Calorific value (MJ/kg) (air-dry basis)	33.50
Free swelling index	9.0
Roga index	86

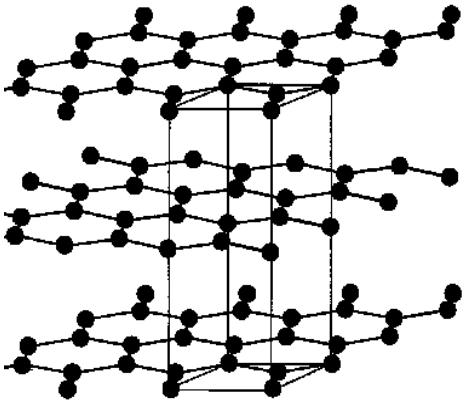

Figure A1: Structure of graphite

Table A.6: Progress of extraction with DMF

	Time (minutes)	**0**	**5**	**10**	**20**	**30**	**45**	**60**	**120**	**180**	**240**	**300**	**360**
Run 1	Mass of Refcoal	0.1159	0.1235	0.1247	0.1164	0.1321	0.1078	0.1005	0.1268	0.1420	0.1231	0.1026	0.1036
	Absorbance @ 600 nm	0.006	0.009	0.011	0.023	0.051	0.084	0.181	0.588	0.875	1.012	1.078	1.102
	Corrected absorbance	0.0052	0.0073	0.0088	0.0198	0.0386	0.0779	0.1801	0.4637	0.6162	0.8221	1.0507	1.0637
Run 2	Mass of Refcoal	0.1231	0.1007	0.1237	0.1136	0.1081	0.1394	0.1304	0.1401	0.1452	0.1352	0.1047	0.1025
	Absorbance @ 600 nm	0.004	0.007	0.012	0.021	0.049	0.098	0.168	0.489	0.822	1.013	1.066	1.108
	Corrected absorbance	0.0032	0.0069	0.0097	0.0185	0.0453	0.0703	0.1288	0.3490	0.5661	0.7493	1.0181	1.0839

Table A.7: Data for the oxidation of the Refcoal

	Time (min)	**0**	**1**	**2**	**3**	**4**	**5**	**6**	**7**	**8**	**9**	**10**	**12**	**15**	**18**	**21**	**24**	**27**	**30**
Exp 1	Volume of oxygen (ml)	0	72	128.6	161.8	179.1	198	215.9	225	239.5	248.1	259.3	272.2	288.9	294.2	296	296.4	296.5	296.7
Exp 2	Volume of oxygen (ml)	0	69	130	157.6	170.9	193.2	216.7	227.3	241.1	253.2	261.7	276.7	290	295.3	297.2	297.8	297.8	297.8
Exp 3	Volume of oxygen (ml)	0	75.3	133.7	164.4	182.9	200	219.7	230.5	243.2	249.1	263.2	275.6	286.4	293.8	292.9	293.3	293.8	294

Exp 4	Volume of oxygen (ml)	0	70.9	127.9	156.7	172.3	192.4	210	223.7	238.6	247.8	255.9	273.2	289.1	295	297.5	296	296.2	296.3
Exp 5	Volume of oxygen (ml)	0	77	131	167.6	187.2	205.5	221.8	235	246.5	256	264	277.5	290.2	295.5	296.2	296.7	296.7	

Table A.8: Infrared spectral regions

Frequencies (cm^{-1})	Band assignment
3 200–3 000	=C-H aromatic stretching mode
3 000–2 800	C-H aliphatic stretching (CH_3, CH_2, CH (tertiary))
1 760–1 640	C=O stretching
1 640–1 540	C=C aromatic and conjugated stretching
910–690	C-H out-of-plane deformations (aromatics ring)
910–840	1 free hydrogen atom
840–770	2 and 3 adjacent hydrogen atoms
770–690	4 and 5 adjacent hydrogen atoms

Table A.9: NMR shift classifications

Type proton	Structure	Chemical shift (ppm)
Cyclopropane	C_3H_6	0.2
Primary	R-C**H**$_3$	0.9
Secondary	R_2-C**H**$_2$	1.3
Tertiary	R3-C-**H**	1.5
Vinylic	C=C-**H**	4.6-5.9
Aromatic	Ar-**H**	6-8.5
Alcohols	**H**-C-OH	3.4-4
Ethers	**H**-C-OR	3.3-4
Esters	RCOO-C-**H**	3.7-4.1
Esters	**H**-C-COOR	2-2.2
Acids	**H**-C-COOH	2-2.6
Carbonyl compounds	**H**-C-C=O	2.-2.7
Hydroxylic	R-C-O**H**	1-5.5
Phenolic	Ar-O**H**	4-12
Carboxylic	RCOO**H**	10.5-12

Table A.10: Operation parameters of X-ray powder diffraction

Radiation	Co
Temperature	25 ºC
Specimen	Flat-plate, rotating (30RPM)
Power setting	45 kV, 40 mA
Soller slit	2º (diffraction beam side)
Divergence slit size	1º
Receiving slits	0.05º
Monochromator	Secondary, graphite
Detector	Scintillation counter
Range of 2θ	10–90º 2θ
Step width	0.008º 2θ
Time per step	5 seconds

Table A.11: Operation parameters of Raman spectroscope

Power at source	200 mW
Excitation line	512.532
Objective lens	x50
Accumulation	2
Condition	Carbonised amorphous carbon
Time	60